The Company of Biologists

RESEARCH ARTICLE

Neuronal changes and cognitive deficits in a multi-hit rat model following cumulative impact of early life stressors

Tiyasha Sarkar, Nisha Patro and Ishan Kumar Patro*

ABSTRACT

Perinatal protein malnourishment (LP) is a leading cause for mental and physical retardation in children from poor socioeconomic conditions. Such malnourished children are vulnerable to additional stressors that may synergistically act to cause neurological disorders in adulthood. In this study, the above mentioned condition was mimicked via a multi-hit rat model in which pups born to LP mothers were co-injected with polyinosinic:polycytidylic acid (Poly I:C; viral mimetic) at postnatal day (PND) 3 and lipopolysaccharide (LPS; bacterial mimetic) at PND 9. Individual exposure of Poly I:C and LPS was also given to LP pups to correlate chronicity of stress. Similar treatments were also given to control pups. Hippocampal cellular apoptosis, β III tubulin catastrophe, altered neuronal profiling and spatial memory impairments were assessed at PND 180, using specific immunohistochemical markers (active caspase 3, β III tubulin, doublecortin), golgi studies and cognitive mazes (Morris water maze and T maze). Increase in cellular apoptosis, loss of dendritic arborization and spatial memory impairments were higher in the multi-hit group, than the single-hit groups. Such impairments observed due to multi-hit stress mimicked conditions similar to many neurological disorders and hence, it is hypothesized that later life neurological disorders might be an outcome of multiple early life hits.

This article has an associated First Person interview with the first author of the paper.

KEY WORDS: Multi-hit, Protein malnourishment, Poly I:C, LPS, Dendritic fragmentation, Spatial memory impairment

INTRODUCTION

Approximately, 4 million neonatal deaths occur every year due to social crisis and 99% of such neonates belong to underdeveloped countries (Målqvist, 2011). A child that survives poverty and social crisis might be at a higher risk for developing later life neurological disorders and hence, the concept of perinatal multi-stress emerges according to which, the children that encounter stress during the perinatal period in the form of malnourishment, viral and bacterial infection, parental separation and other social abuse are vulnerable to the development of neuropsychiatric disorders (Lai and Huang, 2011; Hoeijmakers et al., 2015; Syed and Nemeroff, 2017; Malinovskaya

et al., 2018; Sarkar et al., 2019). The UNICEF data 2018, projects that 50% of deaths among neonates is due to undernutrition, additionally nutritional inadequacy is also attributable to the severity of, and death caused by common infections by delaying the recovery process of the body. Furthermore, the world hunger index indicates that among the different types of malnourishment, protein malnourishment (LP) is predominantly responsible for retardation, delayed physical and mental growth, and child death. Furthermore, viral and bacterial infections are another common issue in already malnourished children belonging to poorer communities because of the unhygienic surroundings in which the children grow (Rytter et al., 2014; Walson and Berkley, 2018). All these stressed conditions can together negatively influence the development and functioning of the central nervous system (CNS) and may be responsible for causing brain adversities in later life.

LP, polyinosinic:polycytidylic acid (Poly I:C; double stranded RNA used to create a viral mimic animal model) and lipopolysaccharide (LPS; bacterial endotoxin, widely used as a bacterial infection agent) are reported to change the neuronal architecture of the fetal brain by destabilizing the synaptic connectivity, leading to a weakening in the process of memory formation, retention and consolidation capacity in rats (Nishi et al., 2014; Yirmiya and Goshen, 2011; Alamy and Bengelloun, 2012; Naik et al., 2015; Sinha et al., 2018). Both malnourishment and immune inflammation during early age play a deleterious role via influencing the cellular integrity of the brain, hence, multiple stress factors together might increase the chances of brain deterioration many fold. Connectivity failure in neuronal circuitry is one of the consequences of early life stress exposure caused by deformities in residential hippocampal neurons, which leads to memory impairment in stressed individuals (Aas et al., 2012) as observed in many neurological disorders like Alzheimer's, schizophrenia, autism, etc. (Singh-Taylor et al., 2014; Justice, 2018).

A decline in the number of viable neurons by caspase mediated apoptotic pathways is common in stress-induced models (Labat-Moleur et al., 1998; Watanabe et al., 2002). Caspases are main executer cysteine proteases, which when activated nucleophilically, attack target proteins resulting in their cleavage and cellular apoptosis. Neuronal degeneration could be due to stress-mediated apoptotic pathways in which activated caspases cleave cytoskeletal and integral cellular proteins, fragmenting and decreasing the overall cell number in the brain. Cytoskeletal proteins are the building blocks of cellular extensions including neuronal arborization and are crucial for stable synapse formation, proper translation, transport and alignment of cytoskeletal subunits (Koleske, 2013). β III tubulin is a subclass of the tubulin family encoded by the *TUBB3* gene in humans, specific to neurons and can be used as a marker for mature neuronal profiling. Neuronal damage can be identified as fragmentation and disruption of β III tubulin subunits, leading to loss of dendritic arborization and connectivity (Poirier et al., 2010; Verstraelen et al., 2017), making the affected individuals prone to developing neurological disorders like Alzheimer's, autism, ADHD and schizophrenia (Bishop et al.,

School of Studies in Neuroscience, Jiwaji University, Gwalior 474011, India.

*Author for correspondence (ishanpatro@gmail.com)

T.S., 0000-0001-6119-3844; N.P., 0000-0002-1578-2055; I.K.P., 0000-0002-6557-6233

Biology Open

2010). Among neuronal sub-types, pyramidal neurons are associated with memory functioning (Kasai et al., 2010), and during memory impairment pyramidal neurons of CA1 (Cornu Ammonis) and CA3 regions of the hippocampus are largely found to be affected (McEwen et al., 2016). The foremost effects of stress on neurons are identified as alterations in the classical morphology of the neurons, which appeared as stubbed, confined or extra-long types. In addition, an overall increase in dendritic fragmentation and neuronal dystrophy, also common in stress-induced brains, leads to a decrease in arborization and synapse formation, subsequent connectivity failure and cell death, which is a common cause for memory impairment and neurological abnormalities (Kulkarni and Firestein, 2012).

Loss of mature neurons also calls for formation of new neurons (Kuhn, 2015; Quadrato et al., 2014). New neurons during adult neurogenesis are formed in the dentate gyrus (DG) in all mammalian species including humans. The newly formed immature neurons subsequently migrate and integrate into the circuitry on demand, i.e. when and where necessary. Naive neurons are initially high in excitability and low in inhibition, but after maturation and integration in the functional layers, they become stable and start extending their processes, forming new arborization and connections with the residential local neurons (Hastings and Gould, 1999; Dieni et al., 2016). Doublecortin (DCX), a neuronal migratory microtubule protein encoded by DCX gene is specific for naive and migratory neurons (Brown et al., 2003). Stress induced changes in adult neurogenesis have been reported by many researchers, but the mechanisms, how it is related to neuronal disintegration and memory impairments has not been well established.

The overall cellular malfunctioning in hippocampus due to various early life stressors may finally lead to memory impairments, which can be considered as onset of neuropsychiatric disorders. The hippocampus is associated with spatial memory impairments (Broadbent et al., 2004; Shrager et al., 2007), which includes both spatial reference and spatial working memory (Niewoehner et al., 2007; Bizon et al., 2012). Spatial reference memory can be differentiated from spatial working memory as the former allows left–right discrimination, whereas the latter is used to keep an account of recent activities like completing a task or understanding a sentence (Cowan, 2014). The hippocampus was initially found to be responsible only for declarative or long-term memory but recent studies have supported the involvement of the hippocampus with working memory retention as well (Jeneson et al., 2011; Leszczynski, 2011; Yee et al., 2014). Such is the need for cognition in normal living conditions that the impairment of cognitive abilities can directly be associated with neuropsychiatric disorders (Lajud and Torner, 2015).

Most stress-oriented studies carried out so far have dealt with a single type of stressor, exposed either during gestational or neonatal periods. Gestational exposure of either Poly I:C or LPS is well known to result in maternal immune activation and development of passive immunity in fetus and neonates. Moreover, maternal immune activation models clearly indicate a link with the development of later life neurological disorders in children. This occurs primarily due to trans-placental passage of cytokines, leading to an increased rate of abortion and decreased litter size in rats (French et al., 2013; Mueller et al., 2019). In the present study maternal immunity was not triggered and the immune activation stressors were exposed neonatally, during which – although the pups were under the influence of maternal immunity via mother's
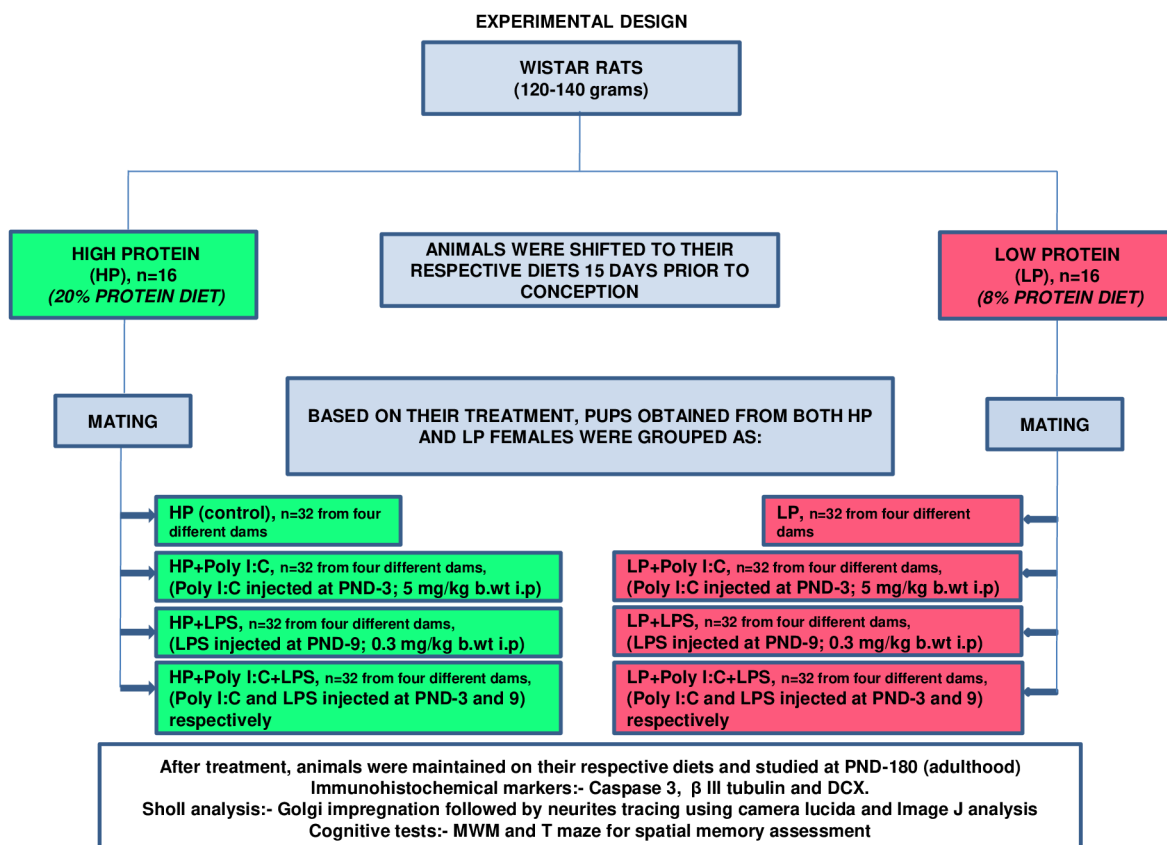

Fig. 1. Representation of the experimental plan in a flow chart.

milk– the transfer of specific antibodies from mother to pups was very unlikely. Developmental windows are prone to every minute change occurring in the environment and hence the developing period is susceptible to multiple stressors, which cumulatively, may act on the developing brain causing later life abnormalities. Moreover, the synergistic and coordinated action of multiple early life stressors on the developing brain is highly challenging and requires our utmost attention. In this study, maternal malnourishment is used to create a stressed uterine environment and the F_1 pups born from both healthy and malnourished mothers were further subjected to viral and bacterial infections with either Poly I:C or LPS, or both simultaneously. As malnourished subjects present high susceptibility to immune infection, such multi-hit models depict the scenario most relatable to that of underdeveloped countries. Thus, in the present study, we tried to investigate the altered morphology and degeneration of neurons in the rat hippocampus, in the context of

memory impairments, using specific immunohistochemical markers and memory oriented cognitive mazes following cumulative exposure of multiple stressors during early life following the experimental design mentioned in Fig. 1.

RESULTS

Early life stressors (LP, Poly I:C and LPS) singularly or in combination induced cell death and cell layer damage in adult rats (PND180), showing cellular changes that are prominent and common in neurodegenerative disorders

Active caspase 3 positive intensely labeled cells were seen in the representative immunohistochemical images of different treated groups (red arrows). In perinatally LP fed animals there was an upregulation of active caspase 3 (Fig. 2E) when compared to high/normal protein (HP) control (Fig. 2A) and when LP animals were administered with single dose of either Poly I:C or LPS (LP+Poly
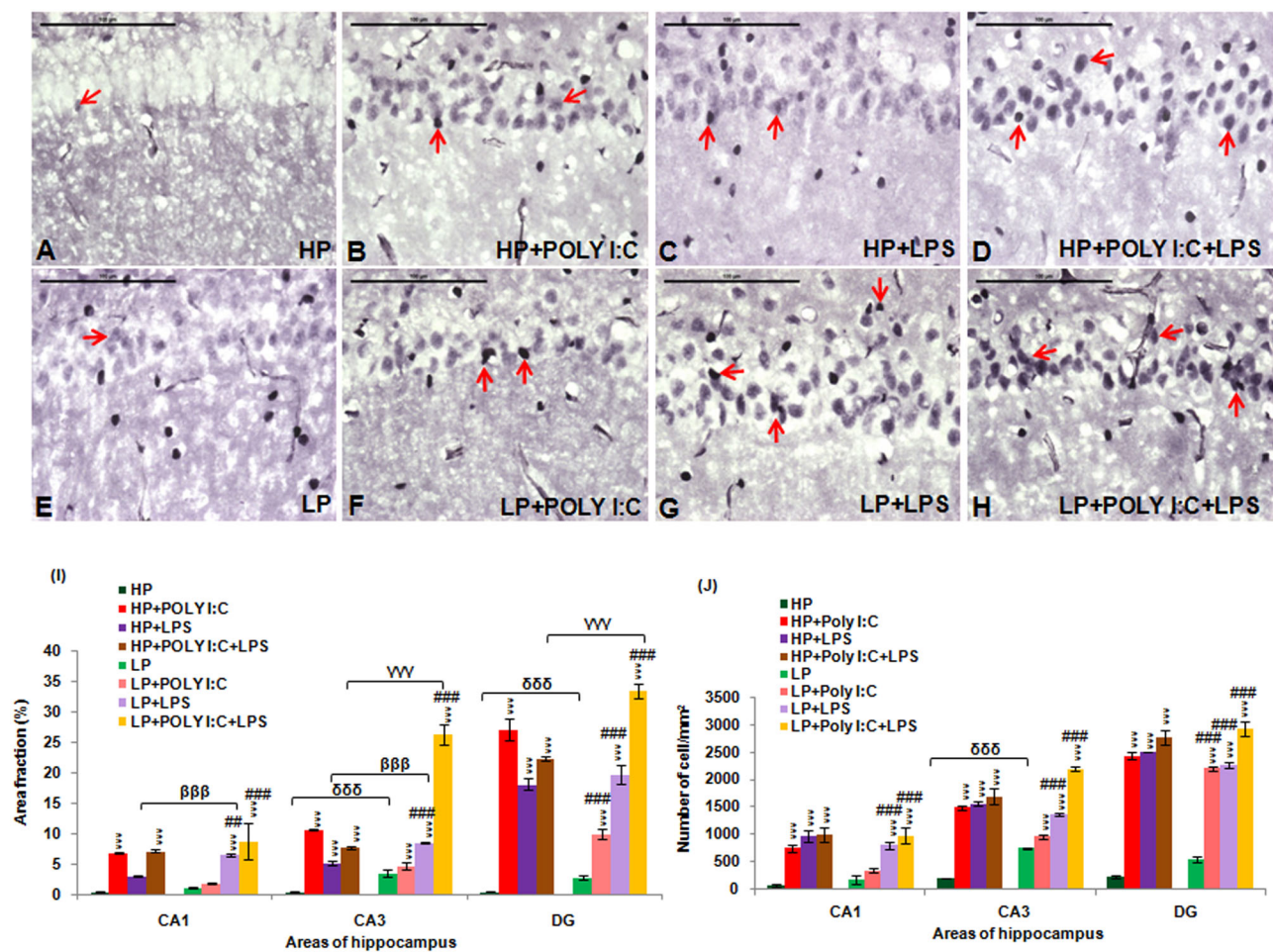

Fig. 2. Active caspase 3 immunolabeled photographs and quantitative analysis of hippocampal sections demonstrating over-expression of activated caspase 3 protein at PND 180 following multi-hit stress. Multi-hit group, i.e. LP+Poly I:C+LPS (H) presented maximum activated caspase 3 activity in comparison to control (A) and rest of the HP and LP treated groups (B–G) (red arrows). When LP and HP animals were subjected to single dose of either Poly I:C or LPS, the caspase 3 expression in LP+Poly I:C (F), LP+LPS (G), HP+Poly I:C (B) and HP+LPS (C) group was found to be higher than HP and LP alone group. (n=6 slides from different animals/group, scale bars: 100 μm). The quantitative analysis of active caspase 3 data (I) also shows maximum upregulation of caspase 3 protein in various hippocampal regions of LP+Poly I:C+LPS animals when compared to control and other treated groups. On administration of single stressor, i.e. either Poly I:C or LPS to both HP and LP animals, HP+Poly I:C, HP+LPS, LP+PolyI:C and LP+LPS animals showed more activation of caspase 3 protein in the different regions of hippocampus when compared to HP and LP alone animals. Cell count graph (J), represents all the active caspase 3 positive cells in different groups. All the regions of hippocampus studied, showed same trend with LP+Poly I:C+LPS group having maximum number of cells, followed by HP+Poly I:C+LPS. Poly I:C and LPS treated HP and LP group also showed increased active caspase 3 positive cells, when compared to HP control and LP alone groups. (n=108 images each area from different slides/group). Values of one- and two-way ANOVA are expressed as mean±s.e.m.; *$P \leq 0.05$, ***$P \leq 0.001$ with respect to HP control; βββ$P \leq 0.001$ with respect to HP+LPS and LP +LPS; ɣɣɣ$P \leq 0.001$ with respect to HP+Poly I:C+LPS and LP+Poly I:C+LPS; δδδ$P \leq 0.001$ with respect to HP and LP and ##$P \leq 0.005$, ###$P \leq 0.001$ with respect to LP alone group.

I:C and LP+LPS), the active caspase 3 expression was further exaggerated (Fig. 2F,G, respectively), increasing the number of cells undergoing apoptosis. Furthermore, when both Poly I:C and LPS were administered simultaneously to LP animals (LP+Poly I:C+LPS group), a vigorous increase in active caspase 3 positivity was recorded (Fig. 2H). Similar treatments were also administered to the HP animals (Fig. 2B–D) but the extent of cellular damage in HP groups was much less as compared to their respective LP groups.

The changes vide supra were further confirmed through the quantitative data (Fig. 2I) with the area fraction of active caspase 3 immunopositivity being highly significant in the LP+Poly I:C+LPS group in the hippocampal regions (CA1, CA3 and DG) when compared with HP control [$F_{(7,856)}$=7.68, $P \leq 0.001$; $F_{(7,856)}$=13.97, $P \leq 0.001$; $F_{(7,856)}$=25.92, $P \leq 0.001$, group wise interaction] and LP alone group [$F_{(3,428)}$=6.92, $P \leq 0.001$; $F_{(3,428)}$=5.3, $P=0.001$; $F_{(3,428)}$=20.86, $P \leq 0.001$, interaction within treatments]. A significant upregulation of caspase 3 in HP and LP animals following single-hit of either Poly I:C or LPS was also observed when compared with HP control and LP alone groups, i.e. HP+Poly I:C in CA1 [$F_{(3,428)}$=5.98, $P \leq 0.001$], CA3 [$F_{(3,428)}$=29.25, $P \leq 0.001$] and DG [$F_{(3,428)}$=23.44, $P \leq 0.001$], LP+Poly I:C in CA3 [$F_{(7,856)}$=12.225, $P \leq 0.001$] and DG [$F_{(7,856)}$=8.445, $P \leq 0.001$; $F_{(3,428)}$=6.39, $P \leq 0.001$], HP+LPS in CA3 ($F_{(3,428)}$=13.608, $P \leq 0.001$) and DG [$F_{(3,428)}$=15.516, $P \leq 0.001$] and LP+LPS in CA1 [$F_{(7,856)}$=5.746, $P \leq 0.001$; $F_{(3,428)}$=4.97, $P=0.013$], CA3 [$F_{(7,856)}$=22.92, $P \leq 0.001$; $F_{(3,428)}$=14.19, $P \leq 0.001$] and DG [$F_{(7,856)}$=16.998, $P \leq 0.001$; $F_{(3,428)}$=14.83, $P \leq 0.001$], respectively. Also, impact of LP diet was observed as on LPS and Poly I:C+LPS exposure, the LP animals reacted more vigorously than the corresponding HP groups and significant differences were found between HP versus LP in CA3 [$F_{(1,642)}$=2.93, $P=0.038$] and DG [$F_{(1,642)}$=3.9, $P \leq 0.001$], HP+LPS versus LP+LPS in CA1 [$F_{(1,642)}$=3.26, $P=0.021$], CA3 [$F_{(1,642)}$=9.36, $P \leq 0.001$] and HP+Poly I:C+LPS versus LP+Poly I:C+LPS in CA3 [$F_{(1,642)}$=6.8, $P \leq 0.001$] and DG [$F_{(1,642)}$=3.6, $P \leq 0.009$].

While the area fraction data gave an idea of the intensity of labeling of active caspase 3 protein in the cells, total number of cells expressing active caspase 3 and those going through apoptosis was determined by counting the number of active caspase 3 positive cells. From the cell count data (Fig. 2J), it was seen that Poly I:C, LPS and Poly I:C+LPS treatment to both HP and LP animals, increased the number of cells expressing the active caspase 3 protein, therefore increasing the number of apoptotic cells in different hippocampal regions (CA1, CA3 and DG). Also, combined exposure of Poly I:C and LPS to both HP and LP animals led to maximum increase in number of apoptotic cells when compared to rest of the groups. Significant differences were found between HP and HP+Poly I:C [$F_{(3,428)}$=7.56, $P \leq 0.001$; $F_{(3,428)}$=18.2, $P \leq 0.001$; $F_{(3,428)}$=29.3, $P \leq 0.001$], HP and HP+LPS [$F_{(3,428)}$=9.9, $P \leq 0.001$; $F_{(3,428)}$=22.75, $P \leq 0.001$; $F_{(3,428)}$=30.1, $P \leq 0.001$], HP and HP+Poly I:C+LPS [$F_{(3,428)}$=10.36, $P \leq 0.001$; $F_{(3,428)}$=25.1, $P \leq 0.001$; $F_{(3,428)}$=33.8, $P \leq 0.001$], HP and LP+LPS [$F_{(7,856)}$=19.63, $P \leq 0.001$; $F_{(7,856)}$=19.63, $P \leq 0.001$; $F_{(7,856)}$=19.2, $P \leq 0.001$], HP and LP+Poly I:C [$F_{(7,856)}$=10.1, $P \leq 0.001$; $F_{(7,856)}$=33.6, $P \leq 0.001$; $F_{(7,856)}$=35.8, $P \leq 0.001$] in CA1, CA3 and DG whereas significant difference between HP and LP [$F_{(1,642)}$=9.2, $P \leq 0.001$, impact of diet] was found in CA3 region and significant difference between HP and LP+Poly I:C [$F_{(7,856)}$=12.8, $P \leq 0.001$; $F_{(7,856)}$=14.2, $P \leq 0.001$], was found in CA3 and DG regions, respectively. Within the LP groups there was also a significant difference in active caspase 3 positive cell number between LP and LP+Poly I:C in DG [$F_{(3,428)}$=10.04, $P \leq 0.001$], LP and LP+LPS [$F_{(3,428)}$=5.935, $P \leq 0.001$; $F_{(3,428)}$=10.34, $P \leq 0.001$; $F_{(3,428)}$=15.06,

$P \leq 0.001$] and LP and LP+Poly I:C+LPS [$F_{(3,428)}$=9.01, $P \leq 0.001$; $F_{(3,428)}$=24.3, $P \leq 0.001$; $F_{(3,428)}$=15.06, $P \leq 0.001$] in CA1, CA3 and DG, respectively.

Catastrophe and downregulation of β III tubulin proteins resulted in fragmentation and loss of dendritic extensions

In the HP control animals, at PND180, the pyramidal neurons were morphologically preserved with apical dendrites, being evenly distributed and oriented in specific directions, devoid of any breakage or fragmentation (green arrows). The compactness of CA layer was also maintained in HP control animals (Fig. 3A). Whereas, in LP+Poly I:C+LPS, i.e. multi-hit group, the orientation of dendritic arbor was disrupted with void areas spotted in between crooked dendritic branches (Fig. 3H, red arrows). Additionally, the pyramidal cell layer was comparatively less dense with structurally altered and damaged neuronal population showing catastrophe of β III tubulin subunits when compared with HP control and similarly treated HP group (Fig. 3D). However, the LP alone group animals also presented a comparatively thin population of dendrites with mild β III tubulin labeling (Fig. 3E) as compared to the HP control group. Single-hit of Poly I:C or LPS also brought changes in the architecture of neurons in both HP (Fig. 3B,C) and LP animals (Fig. 3F,G), which, however, was less than the multi-hit group.

The quantification data of β III tubulin mean area fraction (Fig. 3I) revealed a significant downregulation of β III tubulin following multiple stress with Poly I:C and LPS to LP animals in the sub-regions of hippocampus studied, i.e. CA1 [$F_{(7,856)}$=324.5, $P \leq 0.001$], CA3 [$F_{(7,856)}$=65.3, $P \leq 0.001$; $F_{(3,428)}$=6.63; $P \leq 0.001$] and DG [$F_{(7,856)}$=263.2, $P \leq 0.001$; $F_{(3,428)}$=6.09; $P \leq 0.001$] when compared with HP control (group wise interaction) and LP (interaction within treatments) alone group, respectively (Fig. 3I). Single-hit with either Poly I:C or LPS to both HP and LP animals also led to a significant decrease in β III tubulin density in CA1, CA3 and DG regions when compared with HP control, i.e. HP+Poly I:C [$F_{(3,428)}$=204.63, $P \leq 0.001$; $F_{(3,428)}$=34.2; $P \leq 0.001$; $F_{(3,428)}$=211.3; $P \leq 0.001$], HP+LPS [$F_{(3,428)}$=202.5, $P \leq 0.001$; $F_{(3,428)}$=33.7, $P \leq 0.001$; $F_{(3,428)}$=161.6, $P \leq 0.001$], LP+Poly I:C [$F_{(7,856)}$=252.17; $P \leq 0.001$; $F_{(7,856)}$=60.5; $P \leq 0.001$; $F_{(7,856)}$=252.84, $P \leq 0.001$] and LP+LPS [$F_{(7,856)}$=221.16; $P \leq 0.001$; $F_{(7,856)}$=63.9; $P=0.002$; $F_{(7,856)}$=252.8, $P \leq 0.001$]. In addition, dystrophy of β III tubulin increased in LP+Poly I:C and LP+LPS groups mainly in DG region [$F_{(3,428)}$=5.34, $P \leq 0.001$, $F_{(3,428)}$=5.12, $P \leq 0.001$] when compared with LP alone group, respectively. The impact of LP diet can be seen as significant differences were also observed within the HP and LP alone group in CA1 [$F_{(1,642)}$=8.98, $P \leq 0.001$], CA3 [$F_{(1,642)}$=11.81, $P \leq 0.001$] and DG [$F_{(1,642)}$=7.165, $P \leq 0.001$]; HP+LPS and LP+LPS group in CA3 [$F_{(1,642)}$=6.06, $P \leq 0.001$] and DG [$F_{(1,642)}$=4.2, $P=0.003$]; HP+Poly I:C+LPS and LP+Poly I:C+LPS group in CA1 [$F_{(1,642)}$=3.37, $P=0.017$] and CA3 [$F_{(1,642)}$=6.14, $P \leq 0.001$] regions, showing vulnerability of LP animals on stress exposure.

Early life stress leads to decreased dendritic arborization, and dendritic length, leading to a compromised neuronal profile, as analyzed through golgi impregnation followed by Sholl analysis

Analysis of golgi impregnated sections from various groups demonstrated the altered morphology of hippocampal pyramidal neurons on stress exposure. Fragmented dendrites as seen in β III tubulin labeled images were also observed in images of adult rat pyramidal neurons following single and multi-hit exposures. Acute stress generated in HP animals with single dose of either Poly I:C or
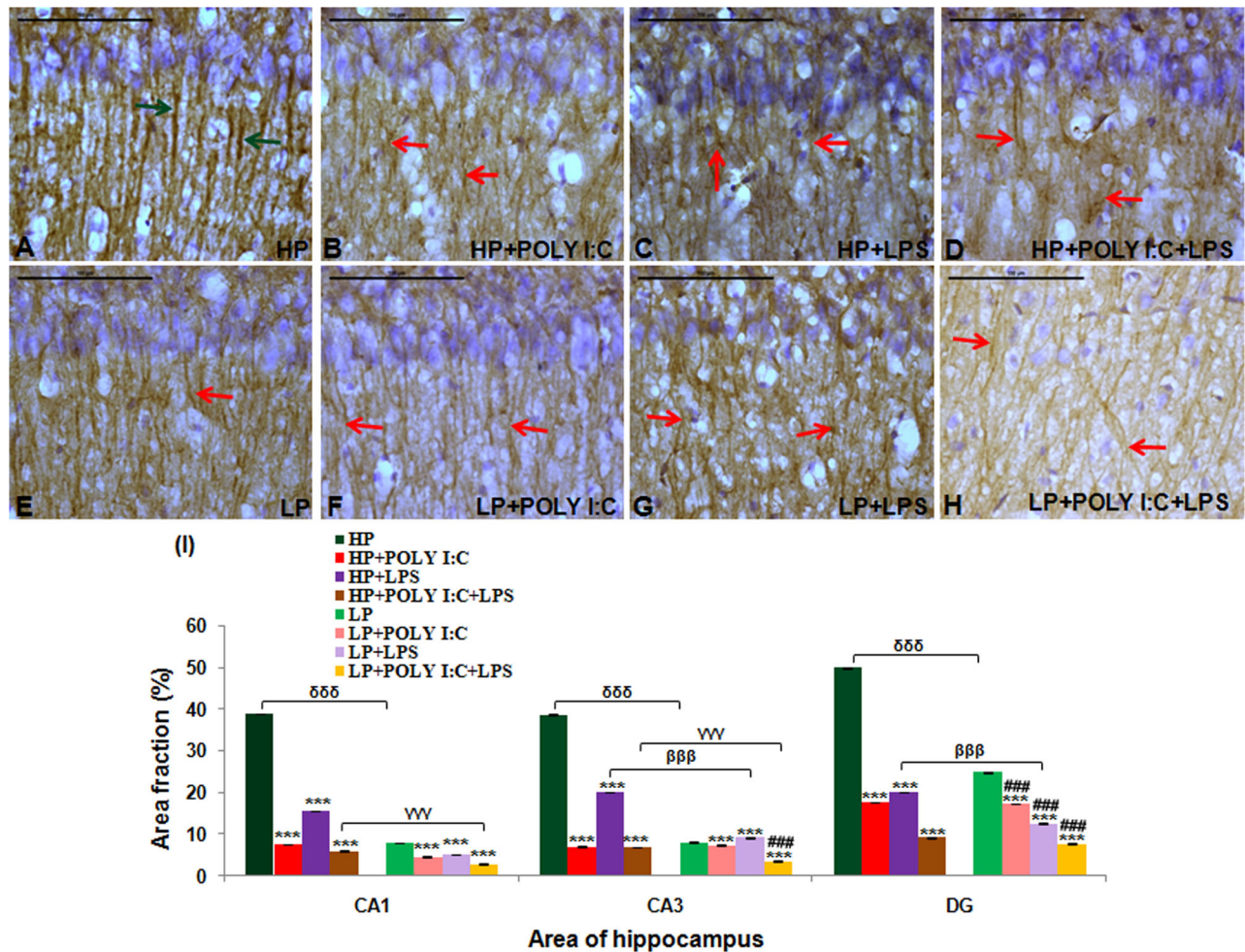
Fig. 3. Light microscope images of β III tubulin labeled hippocampal CA region along with quantification data showing disorientation and misalignment of pyramidal neurons following multi-hit. Systematically orientated and intact neurons with long and continuous dendrites were spotted in adult HP controls (A, green arrows) whereas LP animals on combined exposure of both Poly I:C and LPS (LP+Poly I:C+LPS) showed incorrect neuronal orientation with void spaces in CA region. Their CA layers were loosely packed with tremendous β III tubulin catastrophe (H, red arrows). LP alone (E) and remaining stressed groups (HP+Poly I:C, HP+LPS, LP+Poly I:C, LP+LPS) showed some extent of dendritic damage with LP animals reacting more vigorously to stress when compared to their corresponding HP animals (B–D,F,G), (n=6 slides from different animals/group, scale bars: 100 μm). The quantitative analysis of β III tubulin (I), showed significant decrease in density of β III tubulin in all the three regions of the hippocampus, following multi-hit exposure (LP+Poly I:C+LPS). The remaining LP and HP groups on Poly I:C and LPS treatment also had disintegrated microtubules with the LP animals losing β III tubulin more easily than the similar treated HP animals (n=108 images each area from different slides/group). Values of one- and two-way ANOVA are expressed as mean±s.e.m.; ***$P \leq 0.001$ with respect to HP control; $^{βββ}P \leq 0.001$ with respect to HP+LPS and LP +LPS, $^{γγγ}P \leq 0.001$ with respect to HP+Poly I:C+LPS and LP+Poly I:C+LPS; $^{δδδ}P \leq 0.001$ with respect to HP and LP and $^{###}P \leq 0.001$ with respect to LP alone group.

LPS led to stunting of neurons, decrease in dendritic branches, drooping and haphazardly arranged dendritic arbors in HP+Poly I:C and HP+LPS animals (Fig. 4Cb,c,Eb,c) when compared with HP control (Fig. 4Ab,c). Whereas chronic stress due to prolonged exposure of LP diet or combined administration of Poly I:C and LPS to LP or HP animals led to an abnormal extension of dendrites, which, however, were fragile, incorrectly oriented and drooping (Fig. 4Bb,c,C,Db,c,Fb,c,Gb,Hb,c). Additionally, from the low magnified images of hippocampus it was visible that on chronic stress exposure, i.e. in LP+Poly I:C+LPS animals, the CA layers became indistinct due to increased density and overcrowding of damaged dendrites (Fig. 4Ha).

Sholl analysis on camera lucida traced neuronal images was performed to assess morphometric variation including dendritic arborization and length among treated and control groups. Total number of Sholl circles at an interval of 20 μm gave the length of dendrites, whereas dendritic arborization was calculated from the

mean total number of intersections made by dendrites on the circles. Specifically, pyramidal neurons were chosen for analysis and hence as per the shape of such neurons, numbers of intersecting points in the Sholl circles were at the maximum at 40 μm, which further decreased with increase in the length of the neurons. The histogram was plotted with values of the distance from the soma by X axis and mean number of intersections between dendrites and Sholl circles by Y axis, which gave an idea of the morphometric differences between pyramidal neurons of HP control and other treated groups (Fig. 5). The arborization of dendrites was decreased in LP alone animals, with average dendritic length being confined until 100 μm, when compared with 180 μm long dendrites persistently seen in HP animals. On individual Poly I:C and LPS treatment, the dendritic arborization and length further decreased in HP and LP animals, i.e. HP+Poly I:C (140 μm), HP+LPS (60 μm) and LP+LPS (60 μm). Compensatory increase in dendritic length was observed in LP+Poly I:C animals when compared with LP alone group as the
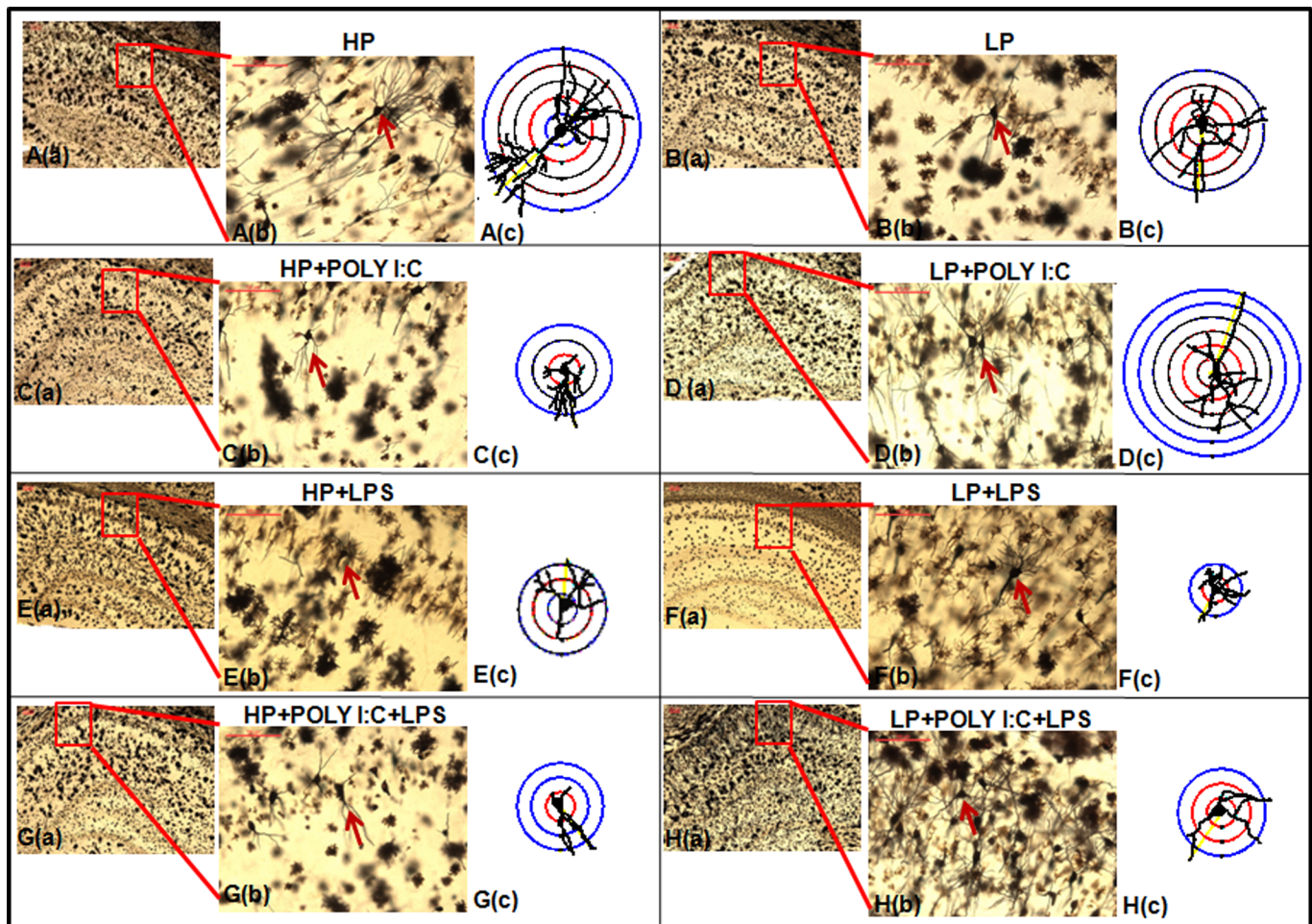
Fig. 4. Microscopic as well as camera lucida traced golgi impregnated images of neurons showing abnormal neuronal morphology on stress exposure. Morphological damage including loss of dendritic branching leading to neuronal stunting and dendritic drooping was seen in chronically stressed LP+Poly I:C+LPS group (Ha–c), when compared with morphologically intact neurons belonging to HP controls (Aa–c). On single-hit with either Poly I:C or LPS, two type of morphological alteration was observed in both HP and LP animals. Some neurons on acute stress were found to be stunted (Ca–c,Ea–c, Fa–c,Ga–c) while others due to chronicity of stress, were observed to compensate for the damage by extending their primary dendrites (Da–c,Ba–c), (n=6 slides from different animals/group, scale bar: 100 μm).

average length of dendrites of LP+Poly I:C group was observed to be 140 μm long. On combined exposure of Poly I:C and LPS to HP and LP animals, i.e. in HP+Poly I:C+LPS and LP+Poly I:C+LPS groups, the average dendritic length and arborization further declined when compared to HP control and LP alone animals (Fig. 5). The statistical data for comparison of mean arborization is tabulated as supplementary data Table S1.

Stress triggered spotting of immature neurons, identified by anti-DCX immunolabeling of naive neurons

Damage induced increase in DCX-positive neurons (arrows) was observed in treated groups. The spotting of DCX-positive neurons in the CA layer was directly proportional to the amount of damage that occurred to residential neurons. Chronic stress due to multiple-hit in LP animals, i.e. LP+Poly I:C+LPS (Figs 6H and 7H) led to a vigorous increase in DCX-positive cells in and around CA layers and DG. Additionally, the DCX-positive cells were not discrete and appeared to be clumped in DG may be because of chronic stress related damage to naive DG neurons. Comparatively, no such increase in DCX-positive cells was seen in HP+Poly I:C+LPS group (Figs 6D and 7D), which could be due to the ability of HP animals to rectify and compensate for chronic immune activated neuronal damage by incorporation of the

naive neurons into the circuitry. HP control animals had very few numbers of DCX-positive neurons in the CA layers (Fig. 6A), but prominent DCX cells were present in the DG notch suggesting healthy adult neurogenesis (Fig. 7A). On the other hand, the LP alone group was seen to have more DCX-expressing cells in the CA layers; however, in the DG, less DCX-positive cells were visible (Figs 6E and 7E). The single exposure of Poly I:C to both HP and LP animals also led to an increase in DCX-positive cells in both the CA layer and DG (Figs 6B,F and 7B,F). No such prominent increase was seen in LPS exposed HP and LP groups (Figs 6C,G and 7C,G).

The morphometric analysis of DCX immunoreactivity in CA1, CA3 and DG (Fig. 7I) revealed the highest upregulation of DCX protein in LP+Poly I:C+LPS group when compared to HP control $[F_{(7,856)}=7.83, P\leq0.001; F_{(7,856)}=45.93, P\leq0.001; F_{(7,856)}=88.74, P\leq0.001]$, LP alone $[F_{(3,428)}=4.89, P=0.003; F_{(3,428)}=6.76, P\leq0.001]$ and HP+Poly I:C+LPS groups $[F_{(1,642)}=8.06, P\leq0.001; F_{(1,642)}=5.78, P\leq0.001; F_{(1,642)}=8.34, P\leq0.001]$. Such an increase in DCX immunopositivity was also seen in the LP+Poly I:C group when compared with HP control and LP alone group in CA1, CA3 and DG $[F_{(7,856)}=28.3, P\leq0.001; F_{(7,856)}=15.9, P\leq0.001; F_{(7,856)}=28.7, P\leq0.001, F_{(3,428)}=4.183, P=0.016; F_{(3,428)}=4.79, P=0.004; F_{(3,428)}=4.009, P=0.02]$ and in HP+Poly I:C group when
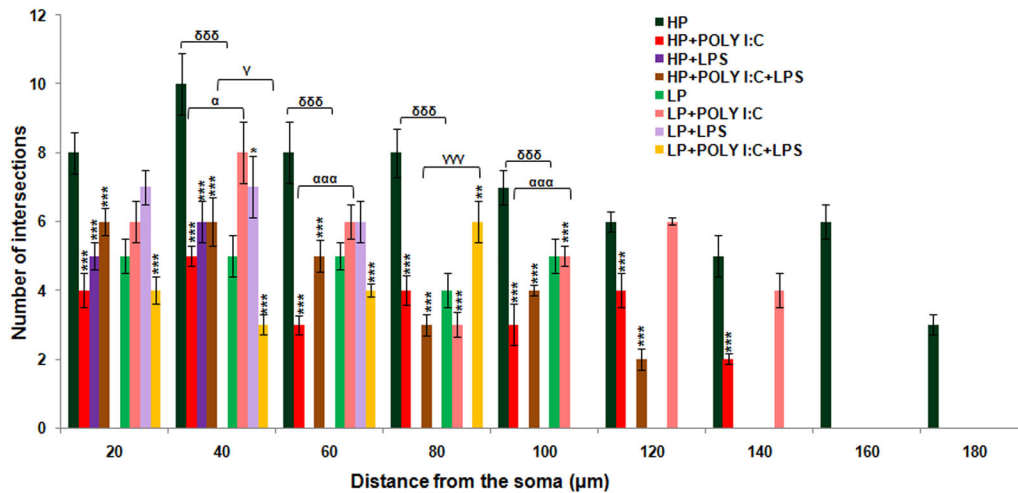
Fig. 5. The histogram shows significant difference in length and arborization between HP control and treated groups on Sholl analysis. The length of the pyramidal neurons denoted as distance from the soma by X axis was affected in all the treated groups. Arborization, denoted as the number of intersections by Y axis were also found to be decreased among treated groups, with minimum arborization seen in LP+Poly I:C+LPS group. (n=108 neurons from six different slides/group). Values of one- and two-way ANOVA are expressed as mean±s.e.m.; *$P{\leq}0.05$, **$P{\leq}0.005$, ***$P{\leq}0.001$ with respect to HP control; $^{\alpha}P{\leq}0.05$, $^{\alpha\alpha\alpha}P{\leq}0.001$ with respect to HP+Poly I:C and LP+Poly I:C; $^{\gamma}P{\leq}0.05$, $^{\gamma\gamma\gamma}P{\leq}0.001$ with respect to HP+Poly I:C+LPS and LP+Poly I:C+LPS and $^{\delta\delta\delta}P{\leq}0.001$ with respect to HP and LP.

compared to HP control in CA1 and DG [$F_{(3,428)}$=16.8, $P{\leq}0.001$; $F_{(3,428)}$=57.7, $P{\leq}0.001$], respectively. Within the group, a significant difference was found between HP control versus LP alone group in CA1 and DG [$F_{(1,642)}$=16.5, $P{\leq}0.001$; $F_{(1,642)}$=47.3, $P{\leq}0.001$], HP+Poly I:C versus LP+Poly I:C in CA1 and CA3 [$F_{(1,642)}$=26.5, $P{\leq}0.001$; $F_{(1,642)}$=37.3, $P{\leq}0.001$] and HP+Poly I:C+LPS versus LP+Poly I:C+LPS in CA1, CA3 and DG [$F_{(1,642)}$=27.83, $P{\leq}0.001$; $F_{(1,642)}$=25.93, $P{\leq}0.001$; $F_{(1,642)}$=18.74, $P{\leq}0.001$].

Impaired spatial memory during Morris water maze (MWM) and T maze task, on exposure to various early life stressors
MWM
Animals were trained to use spatial clues for navigation and localization of escape platform during the MWM task. From the

latency and mean path efficiency graph (Fig. 8I,J), it was noted that due to severe chronicity, the latency was highest and path efficiency was lowest in multi-hit, i.e. LP+Poly I:C+LPS animals when compared with HP control [$F_{(7,88)}$=16.17, $P{\leq}0.001$, $F_{(7,88)}$=11.4, $P{\leq}0.001$] and LP alone group [$F_{(7,88)}$=13.59, $P{\leq}0.001$], which meant that they took more time and followed a more complex path while reaching the escape platform. LP alone animals were also found to have an increased latency and decreased path efficiency depicting impaired spatial memory when compared to HP control ($F_{(1,66)}$=9.54; $P{\leq}0.001$, impact of LP diet] which on further immune activation with either Poly I:C or LPS was heightened as the latency increased and path efficiency decreased in LP+Poly I:C and LP+LPS animals when compared to HP control [$F_{(7,88)}$=5.6; $P{\leq}0.001$; $F_{(7,88)}$=5.8; $P{\leq}0.001$] and similarly treated HP groups,
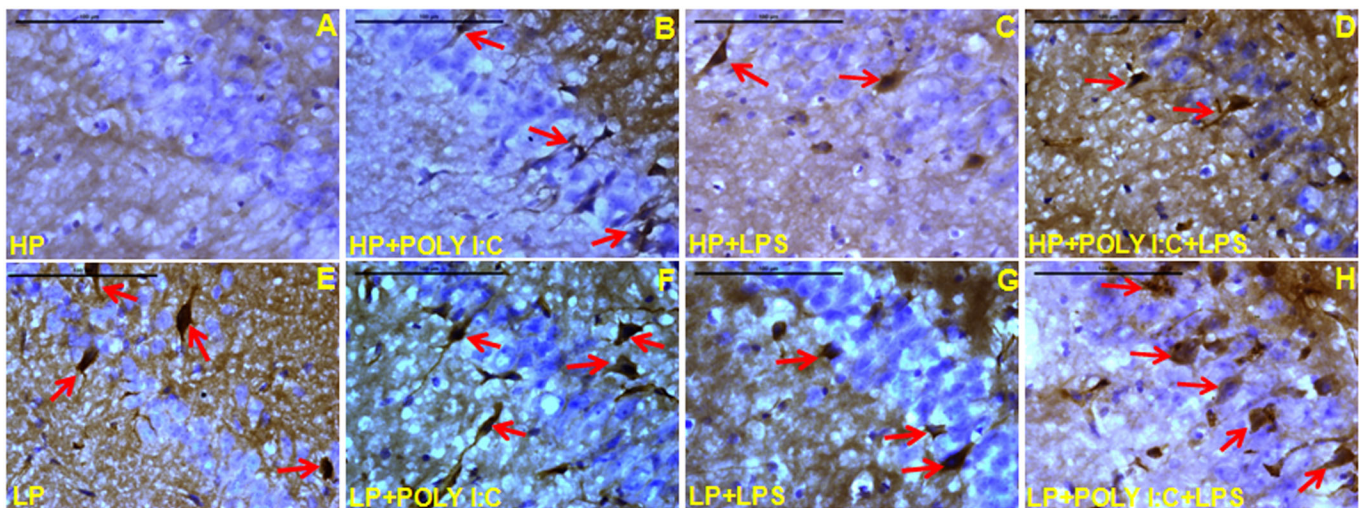

Fig. 6. Microscopic images of hippocampus showing stress dependent increase in DCX expression. Stress induced increase in DCX expressing cells were observed in LP+Poly I:C+LPS group with cells clumped around CA layer (H, red arrows). Poly I:C and LPS were also found to increase DCX expression in both HP and LP animals (B–D,F,G), (red arrows), when compared with HP (A) and LP (E) alone group but again was less than the LP+Poly I:C+LPS group. (n=6 slides from different animals/group, scale bars: 100 μm).
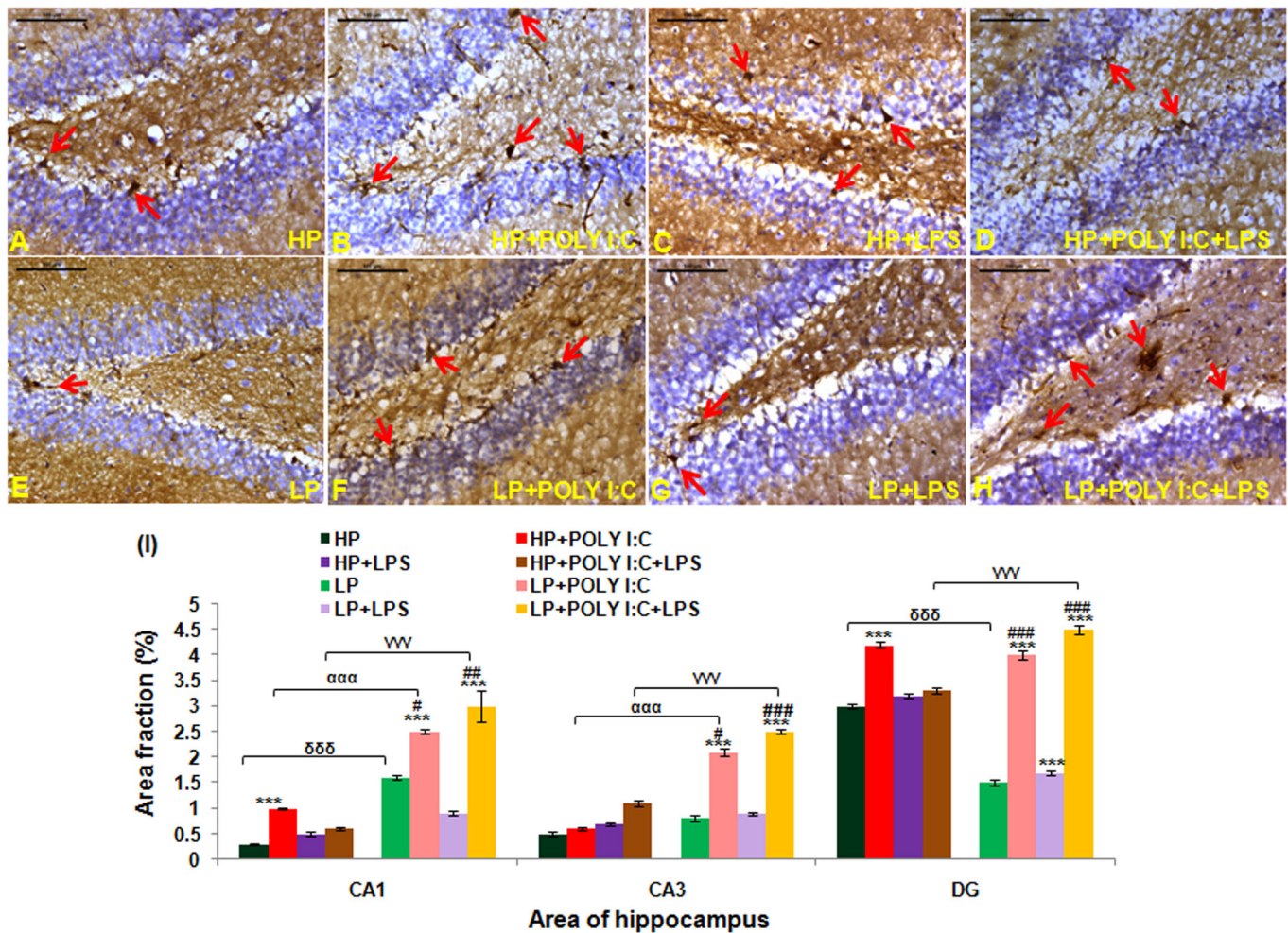
Fig. 7. The photographs of DG and quantification data of DCX protein, showing upregulation of DCX in the multi-hit group. The spotting of DCX positive cells were heightened on combined exposure of Poly I:C and LPS in both HP and LP animals (D, H, red arrows), showing more DCX expressing new neurons when compared with HP (A) and remaining treated groups (B,C,E,F) (*n*=6 slides from different animals/group, scale bars: 100 μm). The graphical representation of mean area fraction (%) of DCX proteins (I) also demonstrated that LP+Poly I:C+LPS group had highest expression of DCX proteins in all the regions of the hippocampus when compared to the other treated groups. (*n*=108 images each area from different slides/group). Values of one- and two-way ANOVA are expressed as mean±s.e.m.; ***$P \leq 0.001$ with respect to HP control; $^{\alpha\alpha\alpha}P \leq 0.001$ with respect to HP+Poly I:C and LP+Poly I:C; $^{\gamma\gamma\gamma}P \leq 0.001$ with respect to HP+Poly I:C+LPS and LP+Poly I:C+LPS; $^{\delta\delta\delta}P \leq 0.001$ with respect to HP and LP and $^{\#}P \leq 0.05$, $^{\#\#}P \leq 0.005$, $^{\#\#\#}P \leq 0.001$ with respect to LP alone group.

i.e. HP+Poly I:C [$F_{(1,66)}$=5.9; $P \leq 0.001$] group. A significant difference in latency were also found between LP, LP+Poly I:C [$F_{(3,44)}$=10.4, $P \leq 0.001$] and LP, LP+LPS groups [$F_{(3,44)}$=12.6, $P \leq 0.001$]. In addition, when percentage of time spent in target quadrant data were analyzed (Fig. 8K), it was seen that HP control group had the longest time spent in the target quadrant to which the platform belongs, avoiding the other zones. HP+Poly I:C, HP+LPS and HP+Poly I:C+LPS had the shortest percentage of time spent denoting poor memory and incapability of the treated groups to spot the quadrant containing the platform. A significant difference was found between HP and HP+Poly I:C+LPS groups [$F_{(3,44)}$=8.25; $P \leq 0.001$]. LP alone group had low percentage of time spent when compared to HP control [$F_{(1,66)}$=7.01; $P \leq 0.001$], which further reduced on Poly I:C, LPS and Poly I:C+LPS exposure [$F_{(3,44)}$=7.2; $P \leq 0.001$, $F_{(3,44)}$=7.9; $P \leq 0.001$, $F_{(3,44)}$=9.4; $P \leq 0.001$] when compared to HP control group. Thus, from the above-mentioned data it can be seen that combination exposure acted synergistically with LP treatment and extravagated the damage in LP animals. However, such effects of multi-hit stress were much less severe

in HP animals, which may be because of their ability to resist or rectify.

From the results of the MWM task, indirect and complex trajectory depicting impaired spatial memory was seen in LP (Fig. 8E) alone, LP+Poly I:C (Fig. 8F), and LP+LPS (Fig. 8G) groups. The HP control animals (Fig. 8A) followed a direct path from the start point to the escape platform, which the treated animals failed to do. The complexity of tracks and impairment of memory increased with the increase in chronicity of stress, hence, the LP+Poly I:C+LPS animals as they took indirect and haphazard paths and reached the escape platform after performing multiple errors when compared with other groups (Fig. 8H). Single or combination exposure of Poly I:C or LPS to HP animals also showed some impairment in path efficiency (Figs 8B–D), but was comparatively less than the respective LP group animals.

T Maze

Alternate baited arm protocol was followed in T maze task to check spatial working memory among all the groups. The mean path
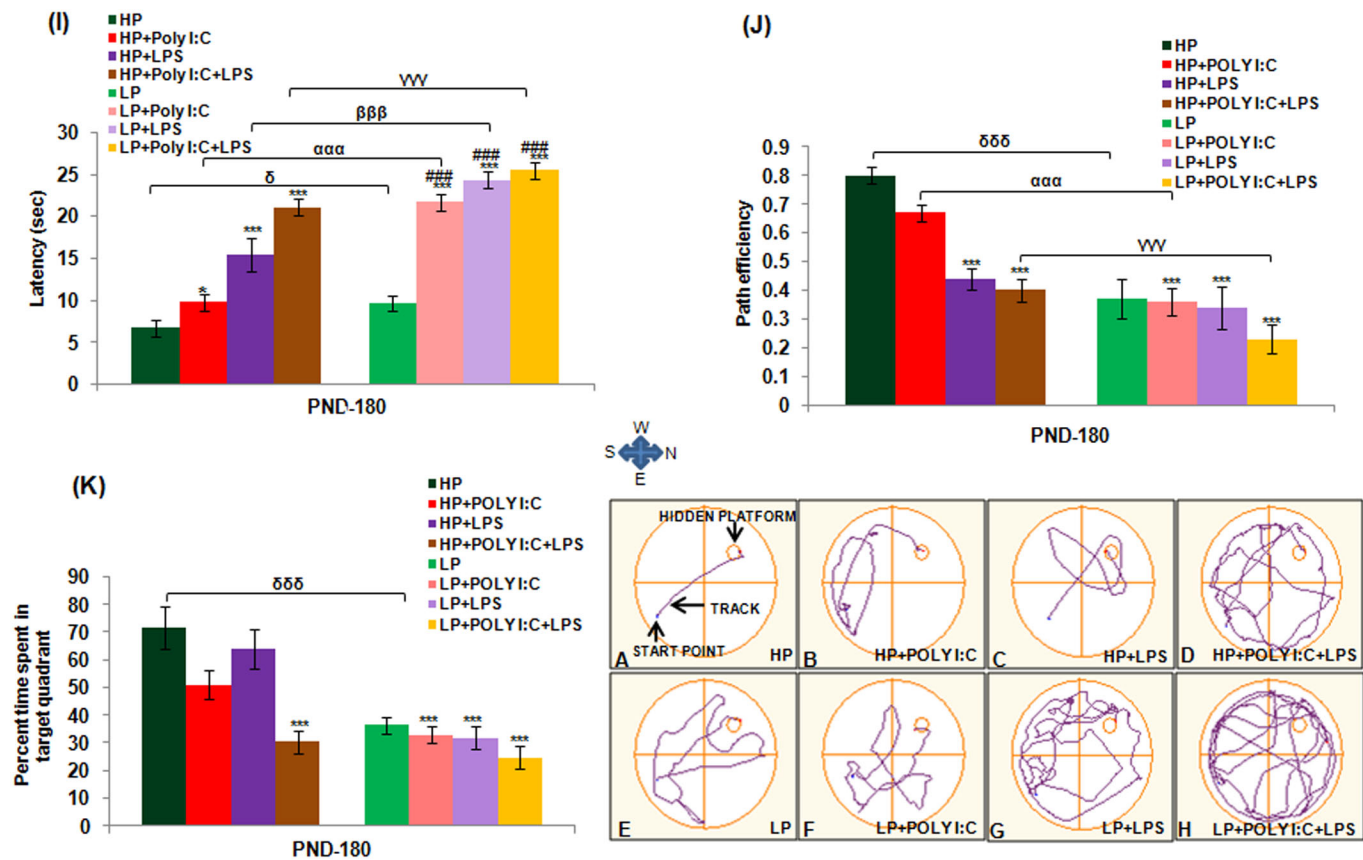
Fig. 8. MWM data showing memory impairment in rats on stress exposure. The track records of animals during MWM task demonstrates maximum memory impairment in LP+Poly I:C+LPS group (H) when compared to HP control (A) and other treated groups (B–G). The LP animals on treatment with either Poly I:C or LPS (F,G) also performed poorly than the HP control (A) and corresponding HP treated group (B,C), (n=12/group). The graphical analysis of mean latency, path efficiency and percent time spent in target quadrant (I–K) depicts memory impairment in HP and LP animals on Poly I:C and LPS administration as the animals belonging to treated groupstook longer time to reach the escape platform, followed complicated trajectory and spent less time in the target quadrant. Maximum deficit was shown by LP+Poly I:C+LPS animals, when compared to rest of the groups. Within the group significant difference was found between HP+Poly I:C and LP+Poly I:C animals, showing that on administration of Poly I:C or LPS, LP animals suffered more damage when compared to HP animals. (n=12/group). Values of one- and two-way ANOVA are expressed as mean±s.e.m.; ***$P \leq 0.001$ with respect to HP control; $\alpha\alpha\alpha$$P \leq 0.001$ with respect to HP+Poly I:C and LP+Poly I:C; $\gamma\gamma\gamma$$P \leq 0.001$ with respect to HP+Poly I:C+LPS and LP+Poly I:C+LPS and $\delta$$P \leq 0.05$,$\delta\delta\delta$$P \leq 0.001$ with respect to HP and LP.

efficiency data were plotted in a graph (Fig. 9I), from which it was interpreted that spatial working memory was impaired following stress. Such spatial memory impairment was seen to be highest in multi-hit group, i.e. LP+Poly I:C+LPS, as the animals were not able to distinguish between left and right arms, and they committed more errors while choosing the correct arm to obtain the reward [$F_{(7,88)}$=9.3; $P \leq 0.001$]. Similar to MWM, the LP alone animals performed less efficiently than HP controls [$F_{(1,66)}$=5.53; $P \leq 0.001$]. On additional treatment with Poly I:C or LPS, the path efficiency depicting spatial working memory further declined in LP animals when compared with HP control [$F_{(7,88)}$=7.57; $P \leq 0.001$; $F_{(7,88)}$=6.3; $P \leq 0.001$], and the impairment in LP+Poly I:C [$F_{(1,66)}$=5.072; $P \leq 0.001$] and LP+LPS and LP+Poly I:C+LPS groups was higher than their HP counterparts.

The results revealed distorted and repeated tracks in treated animals, showing errors while choosing the right baited arm. It was evident from the complex and haphazard tracks of LP+Poly I: C+LPS animals that they had higher impairment in their spatial working memory when compared to other treated groups (Fig. 9H). Moreover, LP (Fig. 9E), LP+Poly I:C (Fig. 9F) and LP+LPS (Fig. 9G) animals also had repeated tracks, showing memory impairment when compared to HP control (Fig. 9A) and similarly

treated HP groups (Fig. 9B,C,D). Lastly, within the HP groups, there was impairment in memory upon treatment with Poly I:C and LPS, either singularly or in combination.

DISCUSSION

The role of perinatal stress as causative factor for neurological disorders like schizophrenia, Alzheimer's, Parkinson's, etc. has been well reported (Huang, 2014; Hoeijmakers et al., 2015; Hohmann et al., 2017). However, the mechanism of action of stressors and the influence of one type of stressor on another still remains unclear. Some of the studies have focused the dual-hit hypothesis according to which, first hit at genetic level during critical developmental periods increases the risk of second-hit, which is generally an environmental insult like infection and nutritional deficiency. Dual-hit exposure may act synergistically and give rise to schizophrenic symptoms in adult individuals (Maynard et al., 2001; Feigenson et al., 2014). However, due to a wide range of stressors and their diverse mode of action, dual-hit hypothesis alone is not sufficient to provide a link between stressors and neurological disorders. This study is the first to address and streamline the events that lead to symptoms seen during CNS malfunctioning in a multi-hit model.
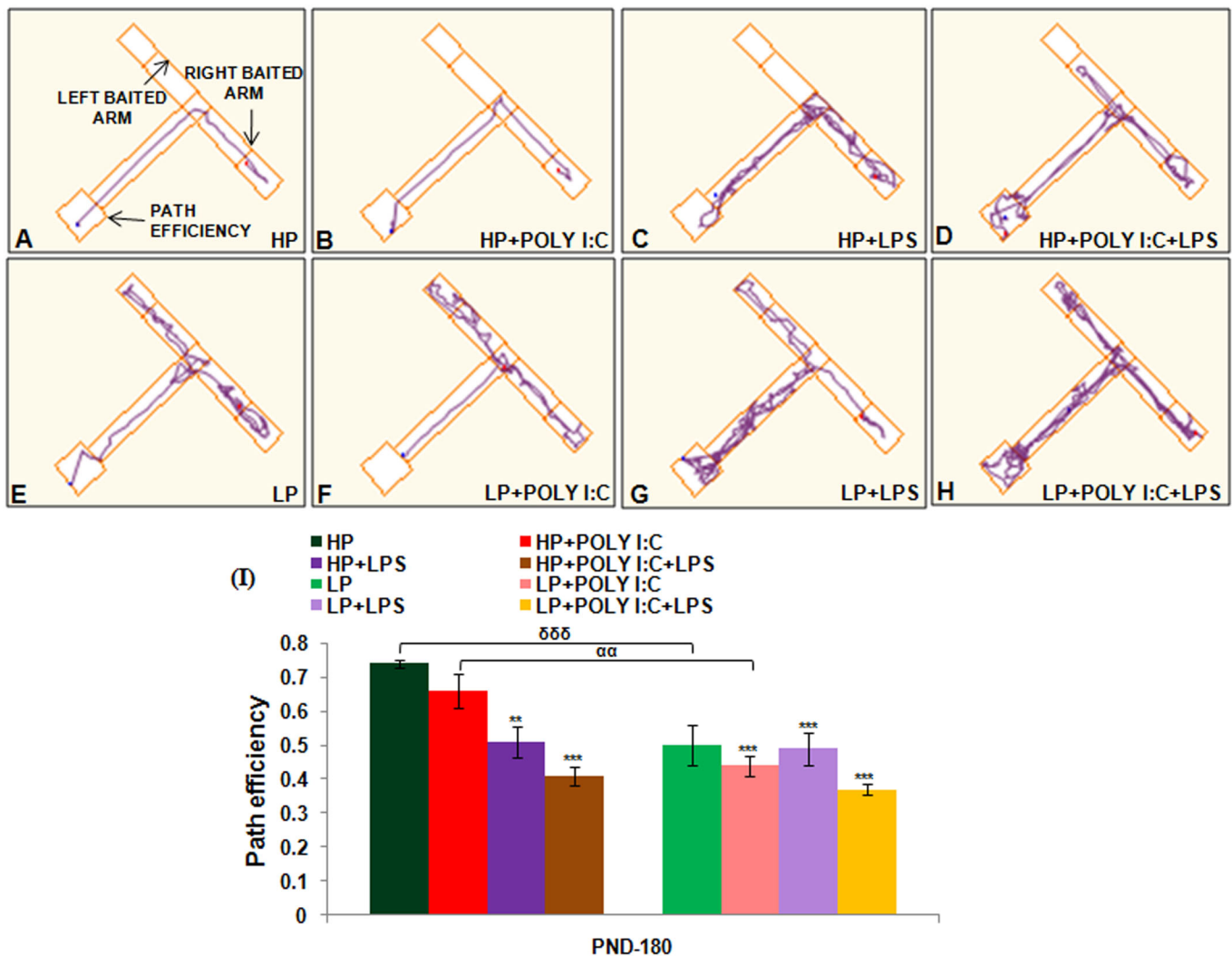
Fig. 9. The mean path efficiency histograms and tracks during T maze task shows maximum decline in path efficiency indicating poor memory in LP+Poly I:C+LPS group. Unavailability of right left discrimination with poor path efficiency in LP+Poly I:C+LPS group (H) is visible from the track records of T maze task. LP alone treated animals also had complex and impaired tracks (E) that further deteriorated on Poly I:C or LPS treatment (F,G). HP animals on similar treatment with Poly I:C and LPS (B–D) also had impaired tracks when compared with the tracks of HP control (A) but, however, the damage in tracks were comparatively lesser than the LP animals, (n=12/group). HP and LP treated single-hit groups showed spatial memory impairment with decrease in path efficiency as seen from the T maze (I) when compared to HP control but damage was chronic in case of multi-hit group when Poly I:C and LPS was administered sequentially in LP animals, i.e. LP+Poly I:C+LPS group. (n=12/group). Values of one- and two-way ANOVA are expressed as mean±s.e.m.; **$P \leq 0.005$, ***$P \leq 0.001$ with respect to controls; $^{\alpha\alpha}P \leq 0.005$, with respect to HP+Poly I:C and LP+Poly I:C and $^{\delta\delta\delta}P \leq 0.001$ with respect to HP and LP.

In this study, perinatally multi-hit animals were found to have the highest active caspase 3 expressions in hippocampus when compared with other groups and additionally, dendrites of such chronically stressed animals also showed active caspase 3 expression depicting their degeneration and neuronal dysfunction. Such upregulation of active caspase 3 could be a reason for low β III expression in multi-hit groups. The multi-hit animals also subsequently exhibited damaged neuronal profile and decreased dendritic arborization, potentially because vigorous active caspase 3 triggered β III tubulin damage. Simultaneous upregulation of DCX protein was also found in DG and CA layers of multi-hit animals with chronic stress, leading to scattering of DCX positive cells in CA layers. Such altered cytoarchitecture of neurons in the hippocampus was finally reflected as the impaired spatial memory in stressed animals, which was directly proportional to the chronicity of stress. Moreover, it was also seen that LP animals were highly prone to infection as they reacted more vigorously to a

subsequent stress exposure when compared to HP animals suggesting, therefore, that the stressors are interdependent and act synergistically, which has been variously hypothesized (Schaible and Kaufmann, 2007; Katona and Katona-Apte, 2008). Apart from the mentioned stressors, studies have also reported that parental suppression and social isolation during early age also leaves a negative impact on the child's brain by increasing cellular death, synaptic malformation and cognitive decline, thus increasing the chance for development of later life neurological disorders, strengthening the link between early life stress exposure and decline of mental health (Callaghan and Tottenham, 2016; Li et al., 2018; Matthews and Tye, 2019).

Active caspase 3 is an apoptotic marker used to study the extent of cellular damage during stress exposure (Mcllwain et al., 2015). Chronic stress in multi-hit (LP+Poly I:C+LPS) animals was found to be responsible for an increase in caspase 3 expression in the hippocampus, which was higher than in the single-hit groups. Such

chronic stress-dependent increase in active caspase 3 protein was also reported in a depressed rat model by Bachis et al. (2008). Restrained stress when combined with forced swim stress was also found to increase the caspase 3 level in the prefrontal cortex of Wistar rats (Zhang et al., 2017). Moreover, Toll-like receptors (TLR) activated by viral and bacterial pathogens along with oxidative stress are also found to be responsible for activating caspases and inducing apoptosis in cells leading to neurodegeneration (Snigdha et al., 2012; Alfonso-Loeches et al., 2013; Sharma et al., 2016). Active caspase 3 dependent neuronal death in case of specific virus-oriented encephalitis, viz., West Nile virus encephalitis and Japanese encephalitis are also being reported (Samuel et al., 2007; Mishra and Basu, 2008). Thus, all the single stress-oriented studies (vide supra) indicate that caspase 3 mediated cell death is a major contributor to neurodegeneration and hence tally with the active caspase 3 data presented in this study. Thus, the vigorous cell death in the hippocampus due to combined exposure of multiple stressors (multi-hit) recorded in this study, suggests a direct correlation with early life multi-hit and chances of occurrence of neurodegenerative and other related disorders.

Beside cell death, activated caspase 3 also causes microtubule distortion leading to dendritic loss and stunting of neurons, prominent in Alzheimer's disease (Troy and Jean, 2015). Stress-dependent damage of the mitochondrial membrane also leads to activation of caspase 3 in dendrites, causing their fragmentation (Mattson et al., 1998; Amelio et al., 2011). Such active caspase 3-labeled dendrites were also seen in chronically stressed multi-hit group in the present study causing their fragmentation. Caspase 3 has also been reported to cleave the tubulin protein causing both axonal and dendritic degeneration (Sokolowski et al., 2014). Thus, the caspase 3 activation during various stress conditions may be a crucial factor leading to β III tubulin degradation.

Multi-hit stress in our study led to an extensive β III tubulin degeneration in neurons, which could be linked to compromised dendritic arborization of neurons and decreased neuronal profiling observed in the multi-hit animals. Such alterations in microtubule dynamics is also observed in cases of Alzheimer's disease as microtubule destabilization is associated with formation of neurofibrillary tangles and aggregation of hyperphosphorylated tau leading to neuronal dystrophy (Brandt and Bakota, 2017). Microtubule instability is also common in other neurodegenerative disorders like Parkinson's disease and amyotrophic lateral sclerosis (Dubey et al., 2015; Salama et al., 2018). Thus, from our β III tubulin data it can be interpreted that multi-hit stress can make an individual prone to neurological disorders as cytoskeletal changes may lead to neurodegeneration, consequently leading to behavioral and cognitive deficits through compromised neuronal arbors.

Stunted neurons due to fragmented and drooping dendrites were common in chronically stressed multi-hit group. Although we have not come across any multi-hit studies so far, our results are well supported by single-hit studies following viral or bacterial infections, stating that the CA1 neurons in rats become architecturally damaged with reduced dendritic length and arborization, further leading to cognitive impairment (Radley et al., 2004; Murmu et al., 2006; Baharnoori et al., 2009; Jurgens et al., 2012). Thus, multi-hit stress could be a major factor that accelerates cellular damage, further causing memory impairment leading to neurodegenerative disorders.

Alongside cellular damage, stressors are also reported to enhance adult neurogenesis in order to compensate for regional damage. In the present study as well, the DCX-positive cells were spotted around CA layers and DG of stressed animals. DCX is reported to be strongly expressed by migrating immature neurons (Kaindl et al., 2006; Klempin et al., 2011; Madhyastha et al., 2013) and in our study, mainly after the multi-hit exposure, DCX expression was upregulated, suggesting an increase in migration of newly generated neurons. Some studies have reported the difference in extent of neurogenesis between sub ventricular (SVZ) and sub granular (SGZ) zone, stating that SVZ regions contain more neural stem cells and with additional amplifying signals, the extent of neurogenesis in SVZ is somewhat higher than SGZ region (Zhu et al., 2014; Ghosh, 2019). However, some studies have also reported a decrease in DCX-positive cells in the hippocampus of rats with chronic stress exposure (Dagytė et al., 2009). This could be because that DCX-positive immature neurons were unable to be incorporated in to the circuitry due to chronicity of stress and hence were prone to degeneration, suggesting that an increase in chronicity decreases the chance of maturation and survival of neurons born as a result of compensation mechanism (Nacher et al., 2004; Lemaire et al., 2006; Naninck et al., 2015). Hence, in our study even with an increase in adult neurogenesis, the cognitive abilities of stressed animals remain impaired in the multi-hit animals showing severe memory loss in both MWM and T maze task, which could be further linked with occurrence of neurodegeneration related disorders in adult animals.

Memory impairment is a hallmark of neurodegenerative disorders, which occurs due to stress dependent altered neuronal circuitry (Esch et al., 2002; Akers et al., 2006; Wen et al., 2017). Early life exposure to stressors like Poly I:C, LPS and perinatal LP individually are well reported to cause memory impairment in rats (Naik et al., 2015; Zakaria et al., 2017; Baghel et al., 2018). However, in the present study the cumulative exposure of all these early life stressors was found to heighten the memory impairments during later life. Thus, it is hypothesized that multi-stress exposure during early life cause chronic damage to spatial memory in LP+Poly I:C+LPS animals via stress dependent caspase 3 activation and β III tubulin catastrophe leading to loss of neuronal connectivity and subsequent neurodegeneration in adult rats.

MATERIALS AND METHODS
Animal husbandry and early life stress induction
Wistar rats were maintained in the animal house facility under controlled physical environment (temperature=25±1°C; humidity=65±2%; light and dark cycle=12 h). Before shifting to the experimental diet, all F_0 animals were given *ad libitum* access to clean drinkable water (reverse osmosis water) and rat pellet feed. 32 virgin females (3 months old, body weight 120–140 gms) were selected and shifted to control, i.e. high protein (HP; 20% protein, n=16) and low protein (LP; 8% protein, n=16) diets, 15 days prior to mating and then maintained on their respective diets throughout gestation and lactation period (isocaloric rat feed, both 8% and 20% protein diets were obtained from National Institute of Nutrition, Hyderabad, India). The day of parturition was noted as postnatal day 0 (PND 0). The F_1 pups from both HP and LP dams were used for creating the following groups. Litter size was adjusted to eight to avoid variation.

Control
HP F_1 pups (n=32, from four different dams) without any treatment were considered as controls. They were maintained with their respective dams and used for various studies at the age of PND 180 (body weight 230±10 gms).

LP model (single stress)
F_1 pups from LP dams (n=32, from four different dams) were used as LP alone group. The animals were maintained in LP diet and used for various studies at the age of PND 180 (body weight 180±10 gms).

Viral infected model in HP and LP groups (HP+Poly I:C and LP+Poly I:C)
Poly I:C (Sigma-Aldrich; St Louis, USA) was injected to mimic a viral infected model. Stock solution was prepared by dissolving 5 mg of Poly I:C

in pre-heated (60°C) TBE buffer (Tris-Borate-EDTA). The solution was mixed properly and stored at 4°C for further use. Equal number of pups (*n*=32, from four different HP as well as LP dams) were injected with Poly I:C (IP) at PND 3 at a dose of 5 mg/kg body weight. The pups were then returned to their respective dams and maintained until used at PND 180 (HP+Poly I:C, body weight 215±10 gms and LP+Poly I:C, body weight 164± 10 gms) according to the experimental plan.

Bacterial infected model in both HP and LP groups (HP+LPS and LP+LPS)

LPS (Sigma-Aldrich, *Escherichia coli*, serotype 0111:B4), was prepared by dissolving 0.3 mg of LPS in 1 ml of PBS (phosphate buffer saline). Similar to Poly I:C treatment, equal number of pups from both HP and LP dams (*n*=32 from four different dams) were injected with LPS (IP) at PND 9 at a dose of 0.3 mg/kg body weight and then returned to their respective dams and maintained till used accordingly at PND 180 (HP+LPS; body weight 220±10 gms and LP+LPS; body weight 173±10 gms).

Viral and bacterial combined infected (multi-hit) model in both HP and LP groups (HP+Poly I:C+LPS and LP+Poly I:C+LPS)

Pups from both HP and LP groups (*n*=32 from four different dams) were injected (IP) with both Poly I:C and LPS at the same dose and postnatal days similar to the viral and bacterial infected HP and LP groups (PND 3 and 9, Dose-5 mg/kg and 0.3 mg/kg body weight, respectively). The animals were then used for various studies at PND 180 (HP+Poly I:C+LPS, body weight 213±10 gms and LP+Poly I:C+LPS; body weight 160±10 gms).

For accurate injection of small volume of LPS or Poly I:C at a constant rate and to ensure complete absorption, Stoelting Nanoinjector and Hamilton microsyringe were used under aseptic conditions. Controls were injected with vehicle alone in correspondence to Poly I:C and LPS exposure. The pups were not anesthetized rather injections were performed by gently holding the pups. The pups were immediately placed with their respective dams for minimal stress. Equal number of male and female rats was used in each experiment as post hoc analysis did not bring out any sex specific differences and the data from both the sexes was combined together and presented as average values. Litter size of eight to nine pups per dam was used to avoid any variation. The overall study consists of eight groups, four from control diet (HP, HP+Poly I:C, HP+LPS, HP+Poly I:C+LPS) and four from LP diet (LP, LP+Poly I:C, LP+LPS, LP+Poly I:C+LPS) and are detailed in Fig. 1.

Perfusion and tissue harvesting for immunocytochemistry

Animals from all the above-mentioned groups (*n*=6/group, from different dams) were anesthetized using diethyl ether and transcardially perfused at PND 180, using pre-chilled PBS (phosphate buffer saline, 0.01 M, pH7.4) followed by 2% paraformaldehyde prepared in 0.01 M phosphate buffer (PB). The brains were carefully dissected out and then post-fixed for 24 h in the same fixative, using immersion fixation technique. The tissues were cryoprotected in sucrose gradients (10%, 20%, 30% sucrose in PB) for consecutive days. The tissues were then sectioned through occipito-temporal region containing hippocampus (14 μm thickness) using a cryotome machine (Leica CM1900, Germany) followed by storage at −20°C for immunohistochemical analysis.

Immunolabeling of active caspase 3 protein using immuno-enzymatic method with nickel enhancement

Brain sections from each group (*n*=6 slides, from different animals and dams/group) were carefully selected and air dried followed by TBS (0.05 M Tris Buffered Saline, pH7.4) washing. Membrane permeabilization was done for 20 min using 0.5% Triton X-100 (Sigma-Aldrich) in TBS. The sections were then washed with TBS, blocked in 1% H_2O_2 (Merck) and incubated with 1% Normal Serum (Vector, PK6200) for 90 min. After non-specific protein blocking, the sections were incubated overnight at 4°C with anti-active caspase 3 antibody (1:1000; Affinity purified rabbit polyclonal, AF835; R&D Systems) diluted in 1% BSA in TBST (TBS+0.5% triton). The next day, the sections were washed in TBS and incubated with secondary antibody (biotin labeled, 1:100 diluted with 1% BSA in TBST; Vector PK6200) for 90 min, followed by washing with TBS and incubation with streptavidin-biotin HRP labeled tertiary antibody for 90 min (SABC,

1:200 diluted in 1% TBST; Vector PK6200). The sections were further washed with TBS and treated with DAB solution for 20 min [0.025% 3, 3′-diaminobenzidine tetrahydrochloride; (Sigma-Aldrich) +2.5% Nickel Sulphate Hexahydrate, (Sigma-Aldrich) +0.06% H_2O_2] for color development and visualization. The reaction was terminated under running tap water and the sections were rinsed with distilled water, dehydrated in alcohol series, cleared in xylene and mounted with distyrene plasticizer xylene (DPX) and stored for image analysis.

Immunolabeling of β III tubulin and DCX proteins at PND 180

Hippocampal neurons expressing β III tubulin and DCX were detected using anti-β III tubulin and anti-DCX antibodies. Separate slides with hippocampal sections from each group (*n*=6 slides from different animals and dams/group) for both independent antibodies, were air dried and washed using PBS. Washing was followed by permeabilization for 20 min using 0.5% Triton X-100 (Sigma-Aldrich) in PBS. The sections were then washed with PBST (0.1% Tween 20 in PBS), blocked in 1% H_2O_2 (Merck) and incubated with 1% normal Serum (Vector, PK6200) for 90 min. After non-specific protein blocking, the sections were incubated overnight at 4°C with primary antibodies [anti-β III tubulin mouse monoclonal, (Sigma-Aldrich) T7816; anti-DCX, guinea pig polyclonal, (Millipore) AB5910] at a dilution of 1:1000 in 1% BSA in PBST (0.5% triton added to PBS). Next day, the sections were washed with PBST for removal of unbound antibody and incubated with secondary antibody (biotin labeled, 1:100 diluted in 1% BSA in PBST; Vector PK6200) for 90 min, followed by washing with PBST and tertiary antibody incubation for 90 min (SABC, 1:200 dilution in 1% PBST; Vector PK6200). The sections were then washed with PBS and treated with DAB solution [0.025% 3, 3′-diaminobenzidine tetrahydrochloride (Sigma-Aldrich) +0.06% H_2O_2] for visualization. The reaction was terminated under running tap water, and sections were counterstained with Hematoxylin (Vector) for proper visualization of the hippocampal layers. The sections were then dehydrated, cleared in xylene, mounted in DPX and stored for image analysis.

Image analysis

For quantitative measurements, images with fixed frame size (21670.9 μm²) and magnification (20X) were grabbed separately for different regions of the hippocampus, using Leica DME 6000 microscope attached to a computer installed with LAS (Leica application suit) software. For quantitative analysis of different regions, data were analyzed separately, 18 images each for CA1, CA3 and DG were collected from a single slide and a total number of six slides from different animals were analyzed for every marker (*n*=108). During antigen density measurement, the percentage and intensity of positively labeled areas (area fraction) within the frame of all the images was individually detected using image quantification module of Leica Qwin software (Version 3.1). The labeled area depicted the presence of positive cells as well the level of expression of the labeled protein by the respective cells. The mean percent area of immunostaining was calculated for CA1, CA3 and DG and was plotted as histograms. For cell count, images from different regions of hippocampus were quantified separately by interactive cell count module of Leica Qwin software (Version 3.1) and the number of cells were counted from each image/frame area and then calculated as number of cells/mm² and plotted as mean cell count (Sharma et al., 2016). Leica Qwin (Version 3.1) software provide a flexibility to specifically consider the positively labeled cell profile in order to avoid variation due to any difference in background staining. The background was kept constant in each image during density measurement and cell quantification to minimize variability due to background staining.

Golgi technique

From each group, animals (*n*=6, belonging to different dams/group) were decapitated at PND 180, followed by dissection and immediate immersion of brain tissues in golgi fixative solution (consists of sodium dichromate, chloral hydrate, formaldehyde, glutaraldehyde and DMSO). The tissues were immersed fixed for 72 h and then treated with 0.75% silver nitrate (Qualigens) solution for minimum 48 h. After complete impregnation, the sections (100 μm thickness) were cut using a Leica Vibratome (VT 1000s). The sections were dehydrated, mounted in DPX and stored for neuronal analysis (Kumar et al., 2013).

Morphological analysis of neurons

Neurons belonging to different animals from each group were traced using camera Lucida, attached to Leica DME microscope (n=36 neurons from six different slides/group). Sholl analysis for dendritic length and arborization was performed for each neuron, using ImageJ freeware software. The number of intersections in each Sholl circle was analyzed for complexity and length of neurites (Baharnoori et al., 2009).

Cognitive experiment for memory analysis at PND 180
(n=12/group from different dams)
MWM

Spatial memory was assessed using MWM (Columbus Instruments) as per the procedure opted by Naik et al., (2015). Initially, the animals were acclimatized and taught to navigate the hidden/escape platform using spatial clues for three consecutive days (four trials for each animal for 120 s). 60 min of gap was given between the trials. During the learning period, if the animals failed to reach the platform, they were manually guided to the escape platform following the shortest and direct path from the start point to the escape platform. On the fourth day, i.e. after 24 h, the animals were subjected to MWM test to locate the escape platform within 120 s. Platform was removed on the fourth day to avoid visual error (probe test). Data were recorded for three trials using a vertical camera connected to an Any Maze software version 4.82. Parameters like the mean path efficiency, i.e. the shortest route taken by the animal to reach the escape platform, latency, i.e. the time taken to reach the escape platform and the percent time spent in the target quadrant (north-west) was analyzed for each and every group.

T Maze

For spatial working memory assessment, T maze from Columbus instrument was used and the protocol was designed according to Nagayach et al., (2014). It is a reward-based test, in which animals were trained and taught to detect the baited arm by remembering previous visited arm. It is a T shaped maze with one start and two reward arms. The animals were also made to learn left–right discrimination in this test. Initially, the animals were acclimatized by placing in the maze and allowing them to explore the whole maze. During training, the animals were placed in the start arm and allowed to arbitrarily choose an arm for 30 s. The animals were then removed and again placed on the start arm, expecting to choose the unexplored arm. The reward was placed at the end of either left or right arm and the position of the reward was changed after every trial. The animals were taught to obtain the reward making minimum effort while choosing the correct arm. Four trials each of 120 s were given to each animal with a gap of 60 min between trials for three consecutive days. On the fourth day, three trials for each animal were performed and the mean path efficiency to reach the reward/baited arm was recorded using a vertical camera attached to an Any Maze software version 4.82.

Statistical analysis

Data were analyzed using one-way ANOVA (for group wise comparison) and two-way ANOVA (for comparison between groups belonging to two independent variables, i.e. diet and treatment) followed by post hoc Holm-Sidak test using Sigma Plot 12. Significance level was preset at $P \leq 0.05$.

The animals were maintained and experimental plan was designed with prior permission from Institutional Animal Ethics Committee of Jiwaji University, Gwalior (M.P.), India.

Compliance with ethical standards

All experiments on rats were performed in accordance with the Institutional Animal Ethics Committee of Jiwaji University and in compliance with National Institutes of Health Guide for the care and use of laboratory animals.

Competing interests
The authors declare no competing or financial interests.

Author contributions
Conceptualization: I.K.P.; Methodology: T.S., N.P.; Validation: N.P.; Formal analysis: T.S., N.P.; Investigation: T.S., N.P.; Data curation: T.S., N.P.; Writing - original draft: T.S., N.P.; Writing - review & editing: T.S., N.P., I.K.P.; Visualization: T.S., N.P.; Supervision: I.K.P.; Project administration: I.K.P.; Funding acquisition: I.K.P.

Supplementary information
Supplementary information available online at
https://bio.biologists.org/lookup/doi/10.1242/bio.054130.supplemental

References

Aas, M., Steen, N. E., Agartz, I., Aminoff, S. R., Lorentzen, S., Sundet, K., Andreassen, O. A. and Melle, I. (2012). Is cognitive impairment following early life stress in severe mental disorders based on specific or general cognitive functioning? *Psychiatry Res.* 198, 495-500. doi:10.1016/j.psychres.2011.12.045

Akers, K. G., Nakazawa, M., Romeo, R. D., Connor, J. A., McEwen, B. S. and Tang, A. C. (2006). Early life modulators and predictors of adult synaptic plasticity. *Eur. J. Neurosci.* 24, 547-554. doi:10.1111/j.1460-9568.2006.04921.x

Alamy, M. and Bengelloun, W. A. (2012). Malnutrition and brain development: an analysis of the effects of inadequate diet during different stages of life in rat. *Neurosci. Biobehav. Rev.* 36, 1463-1480. doi:10.1016/j.neubiorev.2012.03.009

Alfonso-Loeches, S., Pascual, M. and Guerri, C. (2013). Gender differences in alcohol-induced neurotoxicity and brain damage. *Toxicology* 311, 27-34. doi:10.1016/j.tox.2013.03.001

Bachis, A., Cruz, M. I., Nosheny, R. L. and Mocchetti, I. (2008). Chronic unpredictable stress promotes neuronal apoptosis in the cerebral cortex. *Neurosci. Lett.* 442, 104-108. doi:10.1016/j.neulet.2008.06.081

Baghel, M. S., Singh, B., Dhuriya, Y. K., Shukla, R. K., Patro, N., Khanna, V. K., Patro, I. K. and Thakur, M. K. (2018). Postnatal exposure to poly (I: C) impairs learning and memory through changes in synaptic plasticity gene expression in developing rat brain. *Neurobiol. Learn. Mem.* 155, 379-389. doi:10.1016/j.nlm.2018.09.005

Baharnoori, M., Brake, W. G. and Srivastava, L. K. (2009). Prenatal immune challenge induces developmental changes in the morphology of pyramidal neurons of the prefrontal cortex and hippocampus in rats. *Schizophr. Res.* 107, 99-109. doi:10.1016/j.schres.2008.10.003

Bishop, N. A., Lu, T. and Yankner, B. A. (2010). Neural mechanisms of ageing and cognitive decline. *Nature* 464, 529-535. doi:10.1038/nature08983

Bizon, J. L., Foster, T. C., Alexander, G. E. and Glisky, E. L. (2012). Characterizing cognitive aging of working memory and executive function in animal models. *Front. Aging Neurosci.* 12, 4-19. doi:10.3389/fnagi.2012.00019

Brandt, R. and Bakota, L. (2017). Microtubule dynamics and the neurodegenerative triad of Alzheimer's disease: the hidden connection. *J. Neurochem.* 143, 409-417. doi:10.1111/jnc.14011

Broadbent, N. J., Squire, L. R. and Clark, R. E. (2004). Spatial memory, recognition memory, and the hippocampus. *Proc. Natl. Acad. Sci. USA* 101, 14515-14520. doi:10.1073/pnas.0406344101

Brown, J. P., Couillard–Després, S., Cooper–Kuhn, C. M., Winkler, J., Aigner, L. and Kuhn, H. G. (2003). Transient expression of doublecortin during adult neurogenesis. *J. Comp. Neurol.* 467, 1-10. doi:10.1002/cne.10874

Callaghan, B. L. and Tottenham, N. (2016). The neuro-environmental loop of plasticity: a cross-species analysis of parental effects on emotion circuitry development following typical and adverse caregiving. *Neuropsychopharma.* 41, 163-176. doi:10.1038/npp.2015.204

Cowan, N. (2014). Working memory underpins cognitive development, learning, and education. *Educational Psychol. Rev.* 26, 197-223. doi:10.1007/s10648-013-9246-y

Dagytė, G., Van der Zee, E. A., Postema, F., Luiten, P. G. M., Den Boer, J. A., Trentani, A. and Meerlo, P. (2009). Chronic but not acute foot-shock stress leads to temporary suppression of cell proliferation in rat hippocampus. *Neuroscience* 162, 904-913. doi:10.1016/j.neuroscience.2009.05.053

D'amelio, M., Cavallucci, V., Middei, S., Marchetti, C., Pacioni, S., Ferri, A., Diamantini, A., De Zio, D., Carrara, P., Battistini, L. et al. (2011). Caspase-3 triggers early synaptic dysfunction in a mouse model of Alzheimer's disease. *Nat. Neurosci.* 14, 69-76. doi:10.1038/nn.2709

Dieni, C. V., Panichi, R., Aimone, J. B., Kuo, C. T., Wadiche, J. I. and Overstreet-Wadiche, L. (2016). Low excitatory innervation balances high intrinsic excitability of immature dentate neurons. *Nat. Commun.* 7, 1-13. doi:10.1038/ncomms11313

Dubey, J., Ratnakaran, N. and Koushika, S. P. (2015). Neurodegeneration and microtubule dynamics: death by a thousand cuts. *Front. Cell. Neurosci.* 9, 343. doi:10.3389/fncel.2015.00343

Esch, T., Stefano, G. B., Fricchione, G. L. and Benson, H. (2002). The role of stress in neurodegenerative diseases and mental disorders. *Neuroendocrinology Lett.* 23, 199-208.

Feigenson, K. A., Kusnecov, A. W. and Silverstein, S. M. (2014). Inflammation and the two-hit hypothesis of schizophrenia. *Neurosci. Biobehav. Rev.* 38, 72-93. doi:10.1016/j.neubiorev.2013.11.006

French, S. S., Chester, E. M. and Demas, G. E. (2013). Maternal immune activation affects litter success, size and neuroendocrine responses related to behavior in adult offspring. *Physiol. Behav.* **119**, 175-184. doi:10.1016/j.physbeh.2013.06.018

Ghosh, H. S. (2019). Adult neurogenesis and the promise of adult neural stem cells. *J. Exp. Neurosci.* **13**, 1-12. doi:10.1177/1179069519856876

Hastings, N. B. and Gould, E. (1999). Rapid extension of axons into the CA3 region by adult–generated granule cells. *J. Comp. Neurol.* **413**, 146-154. doi:10.1002/(SICI)1096-9861(19991011)413:1<146::AID-CNE10>3.0.CO;2-B

Hoeijmakers, L., Lucassen, P. J. and Korosi, A. (2015). The interplay of early-life stress, nutrition, and immune activation programs adult hippocampal structure and function. *Front. Mol. Neurosci.* **7**, 103. doi:10.3389/fnmol.2014.00103

Hohmann, C. F., Odebode, G., Naidu, L. and Koban, M. (2017). Early life stress alters adult inflammatory responses in a mouse model for depression. *Ann. Psychiatry Ment. Health* **5**, 1095.

Huang, L. T. (2014). Early-life stress impacts the developing hippocampus and primes seizure occurrence: cellular, molecular, and epigenetic mechanisms. *Front. Mol. Neurosci.* **10**, 7-8. doi:10.3389/fnmol.2014.00008

Jeneson, A., Mauldin, K. N., Hopkins, R. O. and Squire, L. R. (2011). The role of the hippocampus in retaining relational information across short delays: the importance of memory load. *Learn. Mem.* **18**, 301-305. doi:10.1101/lm.2010711

Jurgens, H. A., Amancherla, K. and Johnson, R. W. (2012). Influenza infection induces neuroinflammation, alters hippocampal neuron morphology, and impairs cognition in adult mice. *J. Neurosci.* **32**, 3958-3968. doi:10.1523/JNEUROSCI.6389-11.2012

Justice, N. J. (2018). The relationship between stress and Alzheimer's disease. *Neurobiol. Stress* **8**, 127-133. doi:10.1016/j.ynstr.2018.04.002

Kaindl, A. M., Sifringer, M., Zabel, C., Nebrich, G., Wacker, M. A., Felderhoff-Mueser, U., Endesfelder, S., Von Der Hagen, M., Stefovska, V., Klose, J. et al. (2006). Acute and long-term proteome changes induced by oxidative stress in the developing brain. *Cell Death Differ.* **13**, 1097-1109. doi:10.1038/sj.cdd.4401796

Kasai, H., Fukuda, M., Watanabe, S., Hayashi-Takagi, A. and Noguchi, J. (2010). Structural dynamics of dendritic spines in memory and cognition. *Trends Neurosci.* **33**, 121-129. doi:10.1016/j.tins.2010.01.001

Katona, P. and Katona-Apte, J. (2008). The interaction between nutrition and infection. *Clin. Infec. Dis.* **46**, 1582-1588. doi:10.1086/587658

Klempin, F., Kronenberg, G., Cheung, G., Kettenmann, H. and Kempermann, G. (2011). Properties of doublecortin-(DCX)-expressing cells in the piriform cortex compared to the neurogenic dentate gyrus of adult mice. *PLoS ONE* **6**, e25760. doi:10.1371/journal.pone.0025760

Koleske, A. J. (2013). Molecular mechanisms of dendrite stability. *Nat. Rev. Neurosci.* **14**, 536-550. doi:10.1038/nrn3486

Kuhn, H. G. (2015). Control of cell survival in adult mammalian neurogenesis. *Cold. Spring Harbor Perspect. Biol.* **7**, a018895. doi:10.1101/cshperspect.a018895

Kulkarni, V. A. and Firestein, B. L. (2012). The dendritic tree and brain disorders. *Mol. Cell. Neurosci.* **50**, 10-20. doi:10.1016/j.mcn.2012.03.005

Kumar, K., Patro, N. and Patro, I. (2013). Impaired structural and functional development of cerebellum following gestational exposure of deltamethrin in rats: role of reelin. *Cell. Mol. Neurobiol.* **33**, 731-746. doi:10.1007/s10571-013-9942-7

Labat-Moleur, F., Guillermet, C., Lorimier, P., Robert, C., Lantuejoul, S., Brambilla, E. and Negoescu, A. (1998). TUNEL apoptotic cell detection in tissue sections: critical evaluation and improvement. *J. Histochem. Cytochem.* **46**, 327-334. doi:10.1177/002215549804600306

Lai, M.-C. and Huang, L.-T. (2011). Effects of early life stress on neuroendocrine and neurobehavior: mechanisms and implications. *Pediatr. Neonatol.* **52**, 122-129. doi:10.1016/j.pedneo.2011.03.008

Lajud, N. and Torner, L. (2015). Early life stress and hippocampal neurogenesis in the neonate: sexual dimorphism, long term consequences and possible mediators. *Front. Mol. Neurosci.* **8**, 3. doi:10.3389/fnmol.2015.00003

Lemaire, V., Lamarque, S., Le Moal, M., Piazza, P.-V. and Abrous, D. N. (2006). Postnatal stimulation of the pups counteracts prenatal stress-induced deficits in hippocampal neurogenesis. *Biol. Psychiatry.* **59**, 786-792. doi:10.1016/j.biopsych.2005.11.009

Leszczynski, M. (2011). How does hippocampus contribute to working memory processing? *Front. Human Neurosci.* **5**, 168. doi:10.3389/fnhum.2011.00168

Li, N., Cui, L., Song, G., Guo, L., Gu, H., Cao, H., Li, G.-D. and Zhou, Y. (2018). Adolescent isolation interacts with DISC1 point mutation to impair adult social memory and synaptic functions in the hippocampus. *Front. Cell. Neurosci.* **12**, 238. doi:10.3389/fncel.2018.00238

Madhyastha, S., Sekhar, S. and Rao, G. (2013). Resveratrol improves postnatal hippocampal neurogenesis and brain derived neurotrophic factor in prenatally stressed rats. *Int. J. Dev. Neurosci.* **31**, 580-585. doi:10.1016/j.ijdevneu.2013.06.010

Malinovskaya, N. A., Morgun, A. V., Lopatina, O. L., Panina, Y. A., Volkova, V. V., Gasymly, E. L., Taranushenko, T. E. and Salmina, A. B. (2018). Early life stress: consequences for the development of the brain. *Neurosci. Behav. Physiol.* **48**, 233-250. doi:10.1007/s11055-018-0557-9

Målqvist, M. (2011). Neonatal mortality: an invisible and marginalised trauma. *Glob. Health Action* **4**, 5724. doi:10.3402/gha.v4i0.5724

Matthews, G. A. and Tye, K. M. (2019). Neural mechanisms of social homeostasis. *Ann. N. Y. Acad. Sci.* **1457**, 5-25. doi:10.1111/nyas.14016

Mattson, M. P., Keller, J. N. and Begley, J. G. (1998). Evidence for synaptic apoptosis. *Exp. Neurol.* **153**, 35-48. doi:10.1006/exnr.1998.6863

Maynard, T. M., Sikich, L., Lieberman, J. A. and LaMantia, A.-S. (2001). Neural development, cell-cell signaling, and the "two-hit" hypothesis of schizophrenia. *Schizoph. Bull.* **27**, 457-476. doi:10.1093/oxfordjournals.schbul.a006887

McEwen, B. S., Nasca, C. and Gray, J. D. (2016). Stress effects on neuronal structure: hippocampus, amygdala, and prefrontal cortex. *Neuropsychopharmacol.* **41**, 3-23. doi:10.1038/npp.2015.171

McIlwain, D. R., Berger, T. and Mak, T. W. (2015). Caspase functions in cell death and disease. *Cold Spring Harb. Perspect. Biol.* **7**, a008656. doi:10.1101/cshperspect.a026716

Mishra, M. K. and Basu, A. (2008). Minocycline neuroprotects, reduces microglial activation, inhibits caspase 3 induction, and viral replication following Japanese encephalitis. *J. Neurochem.* **105**, 1582-1595. doi:10.1111/j.1471-4159.2008.05238.x

Mueller, F. S., Richetto, J., Hayes, L. N., Zambon, A., Pollak, D. D., Sawa, A., Meyer, U. and Weber-Stadlbauer, U. (2019). Influence of poly (I: C) variability on thermoregulation, immune responses and pregnancy outcomes in mouse models of maternal immune activation. *Brain Behav. Immun.* **80**, 406-418. doi:10.1016/j.bbi.2019.04.019

Murmu, M. S., Salomon, S., Biala, Y., Weinstock, M., Braun, K. and Bock, J. (2006). Changes of spine density and dendritic complexity in the prefrontal cortex in offspring of mothers exposed to stress during pregnancy. *Eur. J. Neurosci.* **24**, 1477-1487. doi:10.1111/j.1460-9568.2006.05024.x

Nacher, J., Pham, K., Gil-Fernandez, V. and McEwen, B. S. (2004). Chronic restraint stress and chronic corticosterone treatment modulate differentially the expression of molecules related to structural plasticity in the adult rat piriform cortex. *Neuroscience* **126**, 503-509. doi:10.1016/j.neuroscience.2004.03.038

Nagayach, A., Patro, N. and Patro, I. (2014). Experimentally induced diabetes causes glial activation, glutamate toxicity and cellular damage leading to changes in motor function. *Front. Cell. Neurosci.* **8**, 355. doi:10.3389/fncel.2014.00355

Naik, A. A., Patro, I. K. and Patro, N. (2015). Slow physical growth, delayed reflex ontogeny, and permanent behavioral as well as cognitive impairments in rats following intra-generational protein malnutrition. *Front. Neurosci.* **9**, 446. doi:10.3389/fnins.2015.00446

Naninck, E. F. G., Hoeijmakers, L., Kakava–Georgiadou, N., Meesters, A., Lazic, S. E., Lucassen, P. J. and Korosi, A. (2015). Chronic early life stress alters developmental and adult neurogenesis and impairs cognitive function in mice. *Hippocampus* **25**, 309-328. doi:10.1002/hipo.22374

Niewoehner, B., Single, F. N., Hvalby, Ø., Jensen, V., MeyerzumAltenBorgloh, S., Seeburg, P. H., Rawlins, J. N. P., Sprengel, R. and Bannerman, D. M. (2007). Impaired spatial working memory but spared spatial reference memory following functional loss of NMDA receptors in the dentate gyrus. *Eur. J. Neurosci.* **25**, 837-846. doi:10.1111/j.1460-9568.2007.05312.x

Nishi, M., Horii-Hayashi, N. and Sasagawa, T. (2014). Effects of early life adverse experiences on the brain: implications from maternal separation models in rodents. *Front. Neurosci.* **8**, 166. doi:10.3389/fnins.2014.00166

Poirier, K., Saillour, Y., Bahi-Buisson, N., Jaglin, X. H., Fallet-Bianco, C., Nabbout, R., Castelnau-Ptakhine, L., Roubertie, A., Attie-Bitach, T., Desguerre, I. et al. (2010). Mutations in the neuronal β-tubulin subunit TUBB3 result in malformation of cortical development and neuronal migration defects. *Hum. Mol. Gen.* **19**, 4462-4473. doi:10.1093/hmg/ddq377

Quadrato, G., Elnaggar, M. Y. and DiGiovanni, S. (2014). Adult neurogenesis in brain repair: cellular plasticity vs. Cellular replacement. *Front. Neurosci.* **8**, 17. doi:10.3389/fnins.2014.00017

Radley, J. J., Sisti, H. M., Hao, J., Rocher, A., McCall, T., Hof, P. R., McEwen, B. S. and Morrison, J. H. (2004). Chronic behavioral stress induces apical dendritic reorganization in pyramidal neurons of the medial prefrontal cortex. *Neuroscience* **125**, 1-6. doi:10.1016/j.neuroscience.2004.01.006

Rytter, M. J., Kolte, L., Briend, A., Friis, H. and Christensen, V. B. (2014). The immune system in children with malnutrition-a systematic review. *PLoS ONE* **9**, e105017. doi:10.1371/journal.pone.0105017

Salama, M., Shalash, A., Magdy, A., Makar, M., Roushdy, T., Elbalkimy, M., Elrassas, H., Elkafrawy, P., Mohamed, W. and Donia, M. B. (2018). Tubulin and Tau: possible targets for diagnosis of Parkinson's and Alzheimer's diseases. *PLOS ONE* **13**, e0196436. doi:10.1371/journal.pone.0196436

Samuel, M. A., Morrey, J. D. and Diamond, M. S. (2007). Caspase 3-dependent cell death of neurons contributes to the pathogenesis of West Nile virus encephalitis. *J. Virol.* **81**, 2614-2623. doi:10.1128/JVI.02311-06

Sarkar, T., Patro, N. and Patro, I. K. (2019). Cumulative multiple early life hits-a potent threat leading to neurological disorders. *Brain Res. Bull.* **147**, 58-68. doi:10.1016/j.brainresbull.2019.02.005

Schaible, U. E. and Kaufmann, S. H. E. (2007). Malnutrition and infection: complex mechanisms and global impacts. *PLoS Med.* **4**, e115. doi:10.1371/journal.pmed.0040115

Sharma, A., Patro, N. and Patro, I. K. (2016). Lipopolysaccharide-induced apoptosis of astrocytes: therapeutic intervention by minocycline. *Cell. Mol. Neurobiol.* **36**, 577-592. doi:10.1007/s10571-015-0238-y

Shrager, Y., Bayley, P. J., Bontempi, B., Hopkins, R. O. and Squire, L. R. (2007). Spatial memory and the human hippocampus. *Proc. Natl. Acad. Sci. USA* **104**, 2961-2296. doi:10.1073/pnas.0611233104

Singh-Taylor, A., Korosi, A., Molet, J., Gunn, B. G. and Baram, T. Z. (2015). Synaptic rewiring of stress-sensitive neurons by early-life experience: a mechanism for resilience? *Neurobiol. Stress* **1**, 109-115. doi:10.1016/j.ynstr. 2014.10.007

Sinha, S., Patro, N. and Patro, I. K. (2018). Maternal protein malnutrition: current and future perspectives of spirulina supplementation in neuroprotection. *Front. Neurosci.* **12**, 966. doi:10.3389/fnins.2018.00966

Snigdha, S., Smith, E. D., Prieto, G. A. and Cotman, C. W. (2012). Caspase-3 activation as a bifurcation point between plasticity and cell death. *Neurosci. Bull.* **28**, 14-24. doi:10.1007/s12264-012-1057-5

Sokolowski, J. D., Gamage, K. K., Heffron, D. S., Leblanc, A. C., Deppmann, C. D. and Mandell, J. W. (2014). Caspase-mediated cleavage of actin and tubulin is a common feature and sensitive marker of axonal degeneration in neural development and injury. *Acta Neuropathol. Commun.* **2**, 16. doi:10.1186/2051-5960-2-16

Syed, S. A. and Nemeroff, C. B. (2017). Early life stress, mood, and anxiety disorders. *Chronic Stress* **1**, 2470547017694461. doi:10.1177/2470547017694461

Troy, C. M. and Jean, Y. Y. (2015). Caspases: therapeutic targets in neurologic disease. *Neurotherapeutics* **12**, 42-48. doi:10.1007/s13311-014-0307-9

Verstraelen, P., Detrez, J. R., Verschuuren, M., Kuijlaars, J., Nuydens, R., Timmermans, J. P. and De-Vos, W. H. (2017). Dysregulation of microtubule stability impairs morphofunctional connectivity in primary neuronal networks. *Front. Cell. Neurosci.* **11**, 173. doi:10.3389/fncel.2017.00173

Walson, J. L. and Berkley, J. A. (2018). The impact of malnutrition on childhood infections. *Curr. Opin. Infect. Dis.* **31**, 231. doi:10.1097/QCO.0000000000000448

Watanabe, M., Hitomi, M., Van Der Wee, K., Rothenberg, F., Fisher, S. A., Zucker, R., Svoboda, K. K. H., Goldsmith, E. C., Heiskanen, K. M. and Nieminen, A.-L. (2002). The pros and cons of apoptosis assays for use in the study of cells, tissues, and organs. *Microsc. Microanal.* **8**, 375-391. doi:10.1017/ S1431927602010346

Wen, M. C., Chan, L. L., Tan, L. C. and Tan, E. K. (2017). Mild cognitive impairment in Parkinson's disease: a distinct clinical entity? *Transl. Neurodegener.* **6**, 24. doi:10.1186/s40035-017-0094-4

Yee, L. T., Hannula, D. E., Tranel, D. and Cohen, N. J. (2014). Short-term retention of relational memory in amnesia revisited: accurate performance depends on hippocampal integrity. *Front. Hum. Neurosci.* **8**, 16. doi:10.3389/fnhum.2014. 00016

Yirmiya, R. and Goshen, I. (2011). Immune modulation of learning, memory, neural plasticity and neurogenesis. *Brain Behav. Immun.* **25**, 181-213. doi:10.1016/j.bbi. 2010.10.015

Zakaria, R., Wan Yaacob, W. M., Othman, Z., Long, I., Ahmad, A. H. and Al-Rahbi, B. (2017). Lipopolysaccharide-induced memory impairment in rats: a model of Alzheimer's disease. *Physiol. Res.* **66**, 553-565. doi:10.33549/ physiolres.933480

Zhang, J. H., Li, M., Han, F. and Shi, Y. X. (2017). Single-prolonged stress induces increased caspase-3 and 9 in mpfcin a rat model of post-traumatic stress disorder. *Biomed. Res.* **28**, 1178-1182.

Zhu, Y., Demidov, O. N., Goh, A. M., Virshup, D. M., Lane, D. P. and Bulavin, D. V. (2014). Phosphatase WIP1 regulates adult neurogenesis and WNT signaling during aging. *J. clin. invest.* **124**, 3263-3273. doi:10.1172/JCI73015